REVIEWS OF MODERN PHYSICS VOLUME 20, NUMBER 1 JANUARY, 1948

Gamma-Radiation from Excited States of Light Nuclei

W. A. FOWLER, C. C. LAURITSEN, AND T. LAURITSEN

Kellogg Radiation Laboratory, California Institute of Technology, Pasadena, California

1. INTRODUCTION

GAMMA-RADIATION emitted in the decay of the excited states of heavy radioactive nuclei has been the subject of experimental and theoretical investigations since the first discovery of natural radioactivity. This radiation has been found to cover the energy range from a few kev up to about 3 Mev, and in this energy range the interaction of the radiation with matter has been extensively studied. As a result, considerable information is now available on the fundamental elementary interactions, the photoelectric effect, the Compton effect, internal conversion, and pair formation. The quantum-mechanical predictions concerning these effects have been verified with a high degree of experimental accuracy. This knowledge of the fundamental interactions makes possible the use of these effects in the study of the spectroscopy of gamma-radiation which in turn leads to information concerning the excited states of the emitting nuclei. An excellent review of this subject has recently appeared in this publication by G. D. Latyshev.[1]

The situation is somewhat different in regard to the gamma-radiation emitted from the excited states of light nuclei. None of the very light nuclei have half-lives long enough to occur in natural radioactivity and, as a result, study of this radiation has been possible only since the discovery in 1919 of the artificial disintegration of light nuclei with naturally radioactive alpha-particles. The development since 1930 of numerous devices, such as the cyclotron and the electrostatic accelerator, for the acceleration of hydrogen nuclei as well as helium nuclei to high energies for use in disintegration experiments has given considerable impetus to the experimental study of this gamma-radiation, and it is, in fact, the results of such investigations which will constitute the major portion of this discussion. Information on the gamma-radiation from light nuclei has also been obtained by use of the neutron as a bombarding particle, although the disintegrations of light nuclei with neutrons have not been as extensively studied as have those of heavy nuclei. The major portion of this discussion will be concerned with investigations in which the proton has been employed as a bombarding agent, since it has been mainly with this particle that direct investigations of gamma-radiation have been made. We note too, at this point, that the illustrative examples are drawn mainly from experimental work done in the Kellogg Radiation Laboratory at the California Institute. It will be clear from the discussion of the results in the last section that the full picture has been the result of experimental and theoretical work in many laboratories.

The situation in the light nuclei is primarily different from that in the heavy nuclei because the energy of the gamma-radiation in general extends to higher values, in fact, up to 17.5 Mev. The experimental study of the elementary interactions in this energy range has by no means been completed. These studies are made difficult because the high energy secondaries produced are capable of magnetic analysis, for example, only through the use of strong magnetic fields extending over considerable regions. Further, the behavior of these secondaries in penetrating matter has not been as extensively studied, the gamma-radiation from light element disintegrations and the cosmic radiation being, until recently, the only source of such secondaries. The recent development of the betatron has furnished a new source.

Nevertheless it has been possible to make some headway in the spectroscopy of the light nuclei and in the determination of the excited states of such nuclei. This is in part due to the fact that, when energetically possible, heavy particles as well as gamma-radiation are emitted by these states. In addition there is reason to believe that

[1] G. D. Latyshev, Rev. Mod. Phys. **19**, 132 (1947).

the quantum-mechanical predictions which have been verified at low energies are valid in this higher energy range. This belief is based on the fact that quantum mechanics has had considerable success in describing the behavior of the still more energetic photons and electrons occurring in the cosmic radiation and in particular in describing theoretically with some exactness the formation of showers which is so characteristic for these components of the cosmic radiation. Furthermore, the studies which have been made of the absorption of gamma-radiation up to 17.5 Mev in energy and of the secondaries produced by this radiation give no reason to believe that the quantum-mechanical calculations on the Compton effect, pair formation, and energy loss by ionization and radiation are in error, although the accuracy of these studies is not very high. In our further discussion we will use the cross sections and other quantities which have been calculated theoretically with some confidence.

2. SOURCES OF THE GAMMA-RADIATION

Before entering into a discussion of certain cases of gamma-radiation emitted from the excited states of light nuclei, we will digress to consider the possible sources from which such radiation can arise. Gamma-radiation is emitted in the transition from one state of a nucleus to another, and so we are primarily concerned with the processes by which excited states of light nuclei can be produced in the laboratory. We note at this point that the energy of the radiation depends on the relative energy values of the two states involved in the transition, i.e.,

$$h\nu = E_1 - E_2, \tag{1}$$

where E_1 is the energy of the initial state, E_2 that of the final state, while the probability of the disintegration per unit time can be expressed as

$$\lambda = f(h\nu) \int \psi_1 q \psi_2^* dv \cdot \int \psi_2 q \psi_1^* dv, \tag{2}$$

where $f(h\nu)$ is a function of the energy of the radiation, q is an operator appropriate to the type of radiation (electric dipole, magnetic dipole, electric quadripole, etc.), and ψ_1 and ψ_2 are the wave functions for the initial and final states. Thus the gamma-radiation leads to information about the energy values of nuclear states and about the coupling between states of the same nucleus or more specifically about the extent of overlapping of the wave functions of these states.

a. Radiation from Compound Nuclei

Excited nuclear states can be produced in a variety of ways in transmutation experiments. The first stage in the interaction of the bombarding particle and the target nucleus is believed to be the formation of a compound nucleus which then disintegrates in any of those ways which are energetically possible and which are not forbidden by strict selection rules. The compound states are more or less characteristic of the nucleus made up of the total number of protons and neutrons in the initial configuration and are relatively independent of their mode of formation.* Because of the decay of the state, its energy has an inherent spread given by

$$\Gamma = \hbar \sum \lambda, \tag{3}$$

where the sum must be taken over all modes of decay. Hence, it is useful to think of the intermediate compound states, which are energetically well defined by the initial experimental situation as "off resonance" modes of motion of those excited states of the compound nucleus which overlap the energy of the intermediate situation. In the simplest cases only one excited state will be involved at a particular bombarding energy. By varying the energy of the incident particle the energy range of a certain state can often be completely covered, the information being obtained in the form of the excitation or yield curve for the various decay processes *versus* the energy of the incident particle. In some cases the same states can be produced with different incident particles and different target nuclei. The yield curves may show very different behavior, but the specific characteristics of the level will also be observable.

One of the competing processes can in almost all cases be gamma-radiation to the ground state of the compound nucleus or to intermediate

* Of course only those compound states will be formed whose spin and parity are consistent with the initial situation and the conservation laws for angular momentum and parity.

states. In only one known case, the pair emitting state of O^{16} at 6.1 Mev, does a strict selection rule prevent gamma-radiation from an excited state of a light nucleus. The yield of the gamma-radiation will be large in those cases where heavy particle decay of the compound nucleus is relatively improbable or forbidden. One process which cannot be forbidden is the re-emission of the incident particle so that the gamma-radiation must in all cases compete with this process. An example is the case**

$$C^{12}+p\rightarrow(N^{13})\begin{cases}\nearrow N^{13}+\gamma \text{ (radiation)}\\ \searrow C^{12}+p \text{ (elastic scattering)},\end{cases} \tag{4}$$

in which only the radiation and elastic scattering processes compete because they alone are energetically possible. Simple calculations based on the masses of the nuclei involved will show that other reactions involving deuterons, alpha-particles, etc., are not possible for low energy protons. Furthermore, inelastic scattering has not been observed, indicating that C^{12} has no low lying excited states. A more general example is the case

$$Li^{7}+p\rightarrow(Be^{8})\begin{cases}\nearrow Be^{8}+\gamma \text{ (radiation)}\\ \nearrow Li^{7}+p \text{ (elastic scattering)}\\ \searrow Li^{7*}+p' \text{ (inelastic scattering)}\\ \searrow \alpha+\alpha \text{ (alpha-particle emission)},\end{cases} \tag{5}$$

where, as, for example, in one state of Be^{8} reached at proton bombarding energies of 440 kev, the radiation and elastic scattering processes alone compete because the alpha-emission is apparently forbidden by a strict selection rule and the inelastic scattering is energetically impossible, while at the same time there are other overlapping states in which the last two processes can also compete as modes of disintegration. It is sometimes convenient to indicate specific excited states of the compound nucleus in the place of the general intermediate situation. In this case care must be taken not to indicate modes of formation or decay which are forbidden for this specific state by strict selection rules.

The emission of deuterons and neutrons as modes of competition is illustrated in the reactions:

$$Be^{9}+p\rightarrow(B^{10})\begin{cases}\nearrow B^{10}+\gamma \text{ (radiation)}\\ \nearrow Be^{9}+p \text{ (elastic scattering)}\\ \rightarrow B^{9}+n \text{ (neutron emission)}\\ \searrow Be^{8}+d \text{ (deuteron emission)}\\ \searrow Li^{6}+\alpha \text{ (alpha-particle emission)}.\end{cases} \tag{6}$$

The energy of the gamma-radiation emitted by the compound nucleus*** will depend on the energy of the initial configuration as determined by the incident particle energy and on the energy of the ground state or intermediate state to which the transition occurs. The gamma-ray energy will thus include the energy equivalent of the mass differences of the nuclei involved plus that portion of the incident particle energy which is not given to translational motion of the compound nucleus. We have****

$$h\nu=(M_0+M_1-M)c^2+\frac{M_0}{M_0+M_1}E_1, \tag{7}$$

where M_0 is the mass of the target nucleus, M the mass of the compound nucleus in the state to which the transition occurs, and M_1 and E_1 are the mass and energy of the incident particle. This equation has been experimentally verified in the case $Be^{9}(p\gamma)B^{10}$, where the mass difference is 6.9 Mev, and Curran *et al.*,[2] have found the maximum energy of the radiation to vary by approximately 0.4 kev with a change in bombarding energy from 400 to 850 kev. It is important to emphasize that this does not indicate that the same states of the nuclei B^{10} are involved at all energies. The results do indicate that the energy of the radiation from the compound situation produced at bombarding energy E_1 will contain a term proportional to E_1. Since the states to which radiation occurs are usually very sharply defined, the energy of the radiation will be uncertain by just the uncertainty in E_1 and not by the uncertainty or width in excited states which overlap E_1.†

** The intermediate compound situations produced by monoenergetic bombarding particles will be designated by placing the nuclear symbol between brackets. These compound situations will, in general, represent numerous excited states of the compound nucleus. Excited states of nuclei will be indicated by asterisks. The particles accompanying excited states of residual nuclei will be indicated by primes. For brevity we will often use the notations $C^{12}(p\gamma)N^{13}$, $C^{12}(pp)C^{12}$, $F^{19}(p\alpha',\gamma)$, etc.

*** Only the gamma-radiation emitted in the first stage of decay of the compound nucleus will be considered in what immediately follows. Subsequent radiation from intermediate states will be discussed under radiation from residual nuclei.

**** We neglect very small Doppler effects.

[2] S. C. Curran, P. I. Dee, and V. Petržílka, Proc. Roy. Soc. **169A**, 269 (1939).

† If E_1 is not near a resonance the intensity may be weak, but for any radiation observed at E_1 with a thin

If we designate integral atomic weights or mass numbers by A and mass excesses by $\delta M = M - A$, we can write

$$h\nu = (\delta M_1 + \delta M_0 - \delta M)c^2 + \frac{A_0}{A} E_1 \qquad (8)$$

for the energy of the gamma-radiation emitted by a compound nucleus. This will also be the energy of excitation of the compound nucleus if we use the M for its ground state. The range in excitation energy which can be studied with a given type of bombarding particles is given approximately by the value of the maximum available energy for these particles (usually $A_0/A \sim 1$). Up to the present time, determinations of excitation curves with high resolution have been made only up to energies of several Mev. Hence detailed knowledge concerning the energy states of a nucleus, as given directly in transmutations where it is the compound nucleus, is confined to a rather limited region of excitation energies. Of course, information on intermediate states is obtained by gamma-ray transitions through these states. The quantity $(\delta M_0 - \delta M)c^2$ for neighboring nuclei can be either positive or negative, and hence the order of magnitude of the excitation of the compound nucleus is given by $\delta M_1 c^2$. Thus with protons and neutrons as bombarding agents one is able to investigate directly the excited states of the compound nucleus which lie near 8 Mev. For compound nuclei such as Be^8, C^{12}, and O^{16} which have small δM relative to those of neighboring nuclei the excitation is considerably higher (17 Mev in the case of Be^8). In deuteron bombardment the excitation is, in general, of the order of 15 Mev, with still higher values in special cases. In alpha-particle bombardment the excitation caused by low energy alpha-particles is, in general, about 3 Mev. The intensity of the reactions for low energy alpha-particles is low, however, and the majority of the experimental results cover excitations of the order of 8 Mev.

The intensity of gamma-radiation from a compound nucleus is proportional to the rate of decay of the nucleus by gamma-emission. Thus by intensity measurements one is able to determine transition probabilities and in turn to obtain information on the nature of the radiation (electric dipole, etc.) and on the character of the states involved in the transition. In addition, the cross section or thin target yield is proportional to the rate of re-emission of the primary particle and inversely proportional to the square of the total rate of decay. The thick target yield contains a term proportional to the ratio of the primary particle rate to the total decay rate. When this ratio is approximately unity, that is, when there is no strong competing process, the thick target intensity will be a maximum given directly by the gamma-ray decay rate. It is only when particle emission is energetically impossible or relatively improbable that gamma-radiation from compound nuclei is strong enough to be observable. We will find the situation to be quite different in the case of gamma-radiation from residual nuclei which is discussed below.

b. Radiation from Residual Nuclei

Gamma-radiation is also emitted by states of the residual nuclei produced in nuclear transmutations. The nuclei remaining after the disintegration of the compound nucleus are often left in excited states. These states are usually stable with respect to heavy particle emission, so that gamma-radiation results as in the reactions:

$$F^{19} + p \rightarrow (Ne^{20}) \begin{cases} \nearrow F^{19} + p & \text{(elastic scattering)} \\ \nearrow O^{16} + \alpha & \text{("long range" alpha-particles)} \\ \searrow O^{16*} + \alpha' & \text{("short range" alpha-particles)} \\ \quad \downarrow & \\ \quad O^{16} + \gamma & \text{(subsequent radiation).} \end{cases} \qquad (9)$$

When the gamma-radiation is from the residual nucleus, the energy of the incident particle will affect the energy of the primary disintegration (α' emission in the example) but not that of the subsequent radiation. This has been demonstrated in the $F^{19}(p\alpha', \gamma)$ reaction by Lauritsen *et al.*,[3] and by Dee *et al.*,[4] who found the quantum energy to be independent of bombarding energy. It is just this evidence which shows conclusively

target, Eq. (7) gives the energy. For a thick target the distribution in energy of the radiation will simulate the thin target excitation curve below E_1. Thus if the resonances below E_1 are narrow, sharp lines corresponding to each resonance will be observed.

[3] T. Lauritsen, C. C. Lauritsen, and W. A. Fowler, Phys. Rev. **59**, 241 (1941).

[4] P. I. Dee, S. C. Curran, and J. E. Strothers, Nature **143**, 759 (1939).

that the radiation is from an excited state of O^{16} and not from the compound nucleus Ne^{20}.

In some cases the residual nucleus can decay further by particle emission. Radiation will then be relatively improbable. A typical case is

$$\begin{array}{ll} & \nearrow B^{11}+p \quad \text{(elastic scattering)} \\ & \nearrow Be^{8}+\alpha \quad \text{(“long range” alpha-emission)} \\ B^{11}+p\rightarrow(C^{12}) & \\ & \searrow Be^{8*}+\alpha' \quad \text{(“short range” alpha-emission)} \\ & \quad\downarrow \\ & \alpha''+\alpha'' \quad \text{(alpha-emission by residual nucleus).} \end{array} \tag{10}$$

It is true that some states of Be^{8} which could be formed by short range alpha-particle emission cannot decay further by disintegration into two alpha-particles because of angular momentum or parity conservation laws. In this case subsequent radiation is to be expected as in (9), but this has not been observed to date.

If the first decay of the compound nucleus is gamma-emission, the residual and compound nucleus are, of course, identical but in different states and one may in fact observe radiation characteristic of all possible transitions from the initial compound state through intermediate states to the ground state. This is observed in the case

$$\begin{array}{ll} & \nearrow C^{12}+\gamma \quad \text{(full energy primary radiation)} \\ B^{11}+p\rightarrow(C^{12}) & \\ & \searrow C^{12*}+\gamma' \quad \text{(lower energy primary radiation)} \\ & \quad\downarrow \\ & C^{12}+\gamma'' \quad \text{(subsequent radiation),} \end{array} \tag{10'}$$

where lines at 16.6, 11.2, and 4.4 Mev are the result of a single transition to the ground state and of a double transition through an intermediate state in C^{12} at 4.4 Mev. In the case of several radiative transitions, only those from the compound state formed in the initial capture will show dependence on the energy of the incident particle (16.6-Mev and 11.2-Mev radiation in the above example).

If the residual nucleus is identical with the target nucleus but in an excited state, the gamma-radiation results from “excitation without capture” and is one phase of the inelastic scattering process, *viz.*,

$$\begin{array}{l} Li^{7}+p\rightarrow(Be^{8})\rightarrow Li^{7*}+p' \quad \text{(inelastic scattering)} \\ \qquad\qquad\downarrow \\ \qquad\qquad Li^{7}+\gamma \quad \text{(radiation).} \end{array} \tag{5'}$$

The energy of excitation of residual nuclei produced in nuclear reactions cannot exceed

$$E_{\max}=(\delta M_1-\delta M_2)c^2 + (\delta M_0-\delta M_3)c^2+(A_0/A)E_1, \tag{11}$$

where the subscripts 2 and 3 designate the particle and the residual nucleus produced in the reaction. Again $(\delta M_0-\delta M_3)c^2$ can be positive or negative, while E_1 is usually small compared to $(\delta M_1-\delta M_2)c^2$, so that in general the determining factor is $(\delta M_1-\delta M_2)c^2$. For (dn) and (dp) reactions this is $\sim$7 Mev, and for $(d\alpha)$ reactions it is $\sim$12 Mev. For $(p\alpha)$ and $(n\alpha)$ reactions it is $\sim$5 Mev. For (pn) or (np) reactions it is small. We note that, in general, the possible excitation of the residual nucleus is somewhat less than that of the compound nucleus.

The intensity of gamma-radiation from a residual nucleus which can decay only by radiation is proportional to the rate of the primary reaction in which the residual nucleus is produced. This is in turn proportional to the decay rate of the compound nucleus by emission of the particle which accompanies the residual nucleus. Since particle emission is relatively more probable than radiation, the intensity of gamma-radiation from residual nuclei produced in a reaction will, in general, be greater than that from the compound nucleus. This is illustrated by the fact that the radiation from $F^{19}(p\alpha', \gamma)$ is more intense than that from such reactions as $Li(p\gamma)$, $Be(p\gamma)$, etc.

In particular, it is certainly more intense than that from the reaction $F^{19}(p\gamma)Ne^{20}$. Radiation from the compound nucleus Ne^{20} has not been observed in this reaction. The gamma-radiation from a residual nucleus will be strong only when it is the only possible mode of decay of the nucleus. When particle emission can compete, the radiation intensity will be of the order of that from compound nuclei.

Radiation transition probabilities are small, so that radiation widths are small ($<$100 electron volts). As a consequence, excited states of residual nuclei which cannot disintegrate with heavy particle emission will give well defined radiation. If the weak radiation competing with heavy particle decay of residual nuclei could be detected it would show a spread in energy equal to the width of the state of the residual nucleus.

c. Radioactive Gamma-Radiation

Nuclei produced in transmutations can be radioactive with electron or positron emission. After the beta-decay the daughter nucleus can be left in an excited state, which, if stable with respect to heavy particle emission, will decay with gamma-emission. In the disintegration of Li^8, transitions occur to excited states of Be^8 which can disintegrate into two alpha-particles and to states for which α-emission is forbidden. In the latter case it has been found recently in this laboratory that gamma-radiation up to 7.5 Mev in energy is emitted but that the number of gamma-rays emitted is considerably less than the number of alpha-particles. Additional investigations of this radiation are being made. In several cases, notably B^{12}, N^{16}, and F^{20}, the beta-ray spectra indicate that not all of the transitions are to the ground states of C^{12}, O^{16}, and Ne^{20}, respectively. Gamma-radiation has been observed[5] in the decay of N^{16} and F^{20} but not in the case of B^{12}. We will not consider radioactive gamma-radiation in detail in this paper.

d. Miscellaneous Sources

In disintegration experiments there are several sources of radiation in addition to the nuclei produced in the disintegration process. These radiations are the 0.51-Mev radiation from the annihilation of positrons, the "bremsstrahlung" given off by fast electrons and positrons in radiative collisions, and the relatively low energy x-radiation generated by the incident particles in being stopped in the target. Some care must be taken not to confuse these radiations with those from the excited states of nuclei. The annihilation radiation has proved exceedingly useful in the calibration of secondary techniques employed in the measurement of gamma-ray energies.

3. MEASUREMENTS ON GAMMA-RADIATION

a. Types of Measurements

Various measurements on gamma-radiation have resulted in information concerning the excited states of nuclei. Early measurements were mainly confined to rough determinations of the yield and energy of the radiation employing, for reasons of intensity, thick targets and the maximum available bombarding energies. With the discovery of pronounced resonances in gamma-ray yields it was appreciated that each of these resonances indicated excited states of the compound nuclei, each with individual characteristics and giving, in general, markedly different yields of radiation and other competing processes and even giving different gamma-ray spectra. As a consequence the accurate determination of excitation curves became of importance, and considerable effort has been expended in numerous laboratories in the construction of accelerating devices with sufficient energy resolution to investigate these excitation curves with accuracy. At the present time proton beams with a spread in energy of less than 300 e-volts at 1 Mev have been obtained.[6,7] For full resolution with such beams, thin targets of less than 0.01-μ thickness must be employed. In this manner the position and width at half-maximum intensity of resonances can be determined. The position of the resonance corrected for factors which depend on the velocity of the incident particle, such as barrier penetration factor, is taken as the mean energy of the excited state. Through the Heisenberg uncertainty principle, the observed width in energy units, properly corrected for beam spread, target thickness, penetration factors, etc., can be used to compute the total decay rate of the state by all possible modes. This is an extremely important experimentally determined characteristic of the state which can be employed theoretically in an attempt to elucidate the fundamental properties of the state.

With the resolution of the different resonances which occur in a reaction it is possible to make measurements of the energy and intensity of the radiation emitted at each resonance. From the energy spectrum of the radiation one learns the coupling of the state with lower lying states. From the intensity of the radiation some information concerning the radiation width or the

[5] D. S. Bayley and H. R. Crane, Phys. Rev. **52**, 604 (1937); H. S. Sommers, Jr. and R. Sherr, Phys. Rev. **69**, 21 (1946); E. Bleuler, P. Scherrer, M. Walter, and W. Zünti, Helv. Phys. Acta **20**, 96 (1947); S. C. Curran and J. E. Strothers, Proc. Camb. Phil. Soc. **36**, 252 (1940).

[6] R. S. Bender, F. C. Shoemaker, and J. L. Powell, Phys. Rev. **71**, 905 (1947).

[7] W. A. Fowler, C. C. Lauritsen, and T. Lauritsen, Phys. Rev. **72**, 746 (1947).

rate of decay of the state by radiation can be obtained. From the radiation width and the energy it may be possible to elucidate the nature of the radiation (electric dipole, etc.) and to determine the angular momentum or other constants of the motion of one of the states involved in the transition, if the corresponding quantity for the other is known.

Gamma-ray measurements are, of course, to be correlated with other sources of information in disintegration experiments. If the radiation is from a compound nucleus, the competing heavy particle modes of disintegration and their rates are important. This is especially true of the resonance scattering.[8] If the radiation is from a residual nucleus it is important to correlate the gamma-ray energies and intensities with those of the heavy particles which have been emitted in the previous step of the reaction. The ultimate experimental objective is complete information concerning the excited states of nuclei. The present experimental results in this regard are summarized in an accompanying paper on "Energy Levels in Light Nuclei."

b. Experimental Arrangements

The ion beam employed in the experimental measurements to be discussed was produced in an electrostatic accelerator which has been previously described.[3,7] In early measurements the beam passed through a 15° magnetic analyzer, and the beam energy was held at a spread of several kilovolts in energy by manual control of the belt charging voltage. In more recent measurements the beam passed through a 90° electrostatic analyzer which automatically controlled the generator potential and impinged on the targets with a spread in energy of less than 300 electron volts at 1 Mev. Points on the excitation curve were obtained at intervals as low as 625 electron volts and in calibration curves at intervals as low as 300 electron volts. No attempt was made to establish an absolute voltage scale. The analyzer was calibrated by measurements of resonances in the $Li^7(p\gamma)$ reaction at 440 kev and in the $F^{19}(p\alpha', \gamma)$ reaction at 862 kev, and it was assumed that the energy of the beam passed by the analyzer was proportional to the voltage across the deflecting plates, which could be measured to one part in 10,000.

The experiments were chiefly concerned with the disintegrations of Li, Be, C, and F by protons. For thick targets, LiOH, polished beryllium metal, Acheson graphite, and polished CaF_2 crystals were employed. For thin lithium targets the metal was deposited on copper backing in vacuum from a small furnace attached to the target assembly. Thin beryllium targets of various thicknesses were employed. The most convenient targets were beryllium foils prepared by Dr. Hugh Bradner of the Radiation Laboratory of the University of California. These foils could be mounted with unsupported areas much larger than the cross section of the proton beam, and thus the radiation from supporting materials (particularly soft x-rays) could be completely eliminated. Numerous foils were used, the thickness varying from 2 to 5×10^{-5} cm (0.037 to 0.092 mg/cm²). For still thinner targets beryllium was evaporated in vacuum and condensed on copper supports. For thin carbon targets paraffin was vaporized in air and condensed on copper supports which could be mounted in the target assembly. For thin fluorine targets, ZnF_2 was evaporated on polished silver targets in vacuum. Throughout these experiments great care was exercised to avoid the effects of the decomposition of targets and the deposition of material by the ion beam. Targets were frequently inspected and cleaned or replaced by new targets. Once yields were established, careful monitoring of the yield was maintained in further investigations.

The gamma-radiation was detected by quartz-fiber electroscopes†† and cylindrical Geiger-Müller counters.††† The electroscopes had a volume of about 180 cc, with a sensitivity as calibrated with radium of 1.2×10^4 ion pairs per cc per division. The wall of the counters weighed 30 mg/cm², the cathode was a thin silver deposit on the glass wall, and the sensitive area was 7.5×1.8 cm or 14 sq. cm. In coincidence measurements of the range of the secondaries produced by the gamma-radiation three counters

[8] E. C. Creutz, Phys. Rev. **55**, 819 (1939).

†† Produced by Fred C. Henson Company, Pasadena, California.

††† Produced by Radiation Counter Laboratories, Chicago, Illinois.

were employed. The secondaries were first counted by a single counter separated from the target tube only by the material used as converter, i.e., the material from which the secondaries were ejected by the gamma-radiation. Two counters operated in parallel completed the coincidence circuit and were separated by a distance somewhat greater than the maximum amount of absorber used to determine the range of the secondaries. The target and counter arrangement was surrounded by a lead covered wooden box which served as a shield against external radiation and gave minimum backscattering for the radiation leaving the target. Typical arrangements are shown schematically in Figs. 7 and 8. In early measurements of excitation curves two electroscopes were employed, one unshielded from the target and the second surrounded by 3 mm of lead. In this way it was possible to differentiate the excitation curve for hard and soft radiation. In later measurements the single counter and the coincidence counters with absorber in place served the same purpose. In intensity measurements two counters and two electroscopes were employed, one set of counter and electroscope with aluminum walls and the other with lead. The use of a cloud chamber in energy measurements of the radiation has been described in detail previously.[3] The beam was well collimated by a lead collimator and passed from target into the chamber through a minimum of structural material. Pairs and electrons were produced in lead and carbon laminae placed across the chamber normal to the radiation. Helmholtz coils around the chamber produced a magnetic field in which the secondaries tracks were curved. The momentum of these secondaries could be determined from the product of the radius of curvature of the track and the magnetic field.

4. THE EXCITATION CURVES

Excitation curves for the reactions $Li^7(p\gamma)$, $Be^9(p\gamma)$, $C^{12}(p\gamma)$, $C^{13}(p\gamma)$, and $F^{19}(p\alpha', \gamma)$ are shown in Figs. 1, 2, 3, and 4. It is convenient to discuss those for $Be^9(p\gamma)$ first. We note at this point only that the basic energy calibration of the proton beam was obtained from the $Li^7(p\gamma)$ curve in Fig. 1. Excitation curves with high resolution for $Be^9(p\gamma)$ were first obtained by

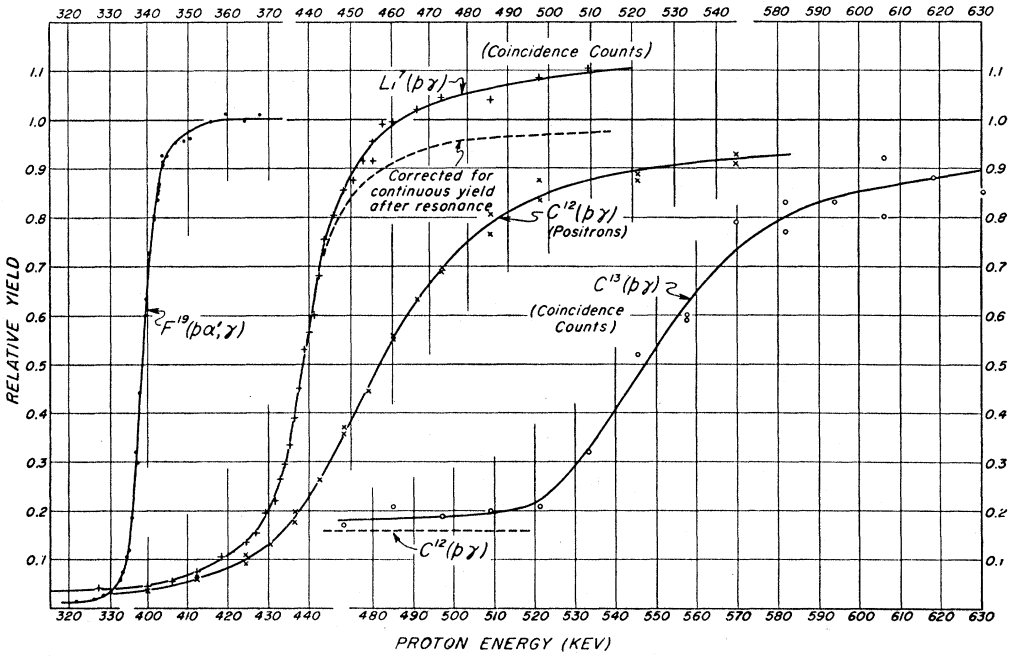

FIG. 1. Thick target excitation curves for the reactions $Li^7(p\gamma)$, $C^{12}(p\gamma)$, $C^{13}(p\gamma)$, and $F^{19}(p\alpha', \gamma)$. In the case of the $C^{12}(p\gamma)$ reaction the positrons from the beta-decay of the residual nucleus, N^{13}, were observed.

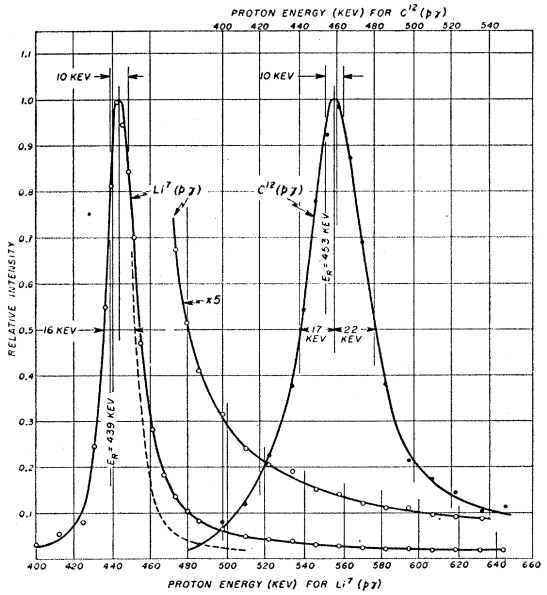

FIG. 2. Thin target excitation curves for the reactions $Li^7(p\gamma)$ and $C^{12}(p\gamma)$. The loss of energy of the incident protons in the targets was approximately 10 kev. The indicated resonance energies at 439 kev and 453 kev were determined from the thick target curves of Fig. 1.

Hushley[9] who found two strong resonances near 1-Mev bombarding energy. These resonances showed very different widths, that at 975 kev being considerably broader than that at 1060 kev. We have attempted to extend Hushley's finding regarding these two resonances. No attempt was made to investigate in detail the weak resonances at 860, 1130, and 1360 kev found by Hushley. We have not observed evidence for these weak resonances consistently from beryllium targets, and they may be due to contamination. It is known that the $F(p\alpha', \gamma)$ reaction gives very large gamma-ray yields at 862 and 1363 kev.

We shall discuss at this point only the width, position, and relative yield of the resonances, leaving the discussion of the absolute yield until after discussion of the energy of the radiation, which enters into the absolute yield determination. As will be noted below, our determinations of the resonance energies yield the values 988 and 1077 kev.

From Fig. 3 it is clear that the resonance just below 1 Mev has considerable width. No resolution into more than one component was observed in these measurements which were taken with points separated by 6-kev intervals. In the case of the lower curve of Fig. 3 which was taken with the thinnest available foil, we have fitted the Breit-Wigner dispersion curve[10] to the observed points. In places where this curve deviates considerably from the observed points, as at the 860- and 1077-kev resonances and above 1.1 Mev, it is indicated by a dashed line. In calculating this curve we have employed only the resonance denominator term (see Eq. (13) below) and have neglected the small variation with energy of the wave-length and barrier penetration factors for the protons. On the low energy side of the resonance the fit is good, extending down to four half-widths from resonance (not completely shown in Fig. 3). The deviation on the high energy side may be due to neglect of the factors indicated above, but is most probably due to the onset of a weak broad resonance centered about ~1.4 Mev. That the radiation of essentially constant yield observed from 1.1 to 1.4 Mev is due to beryllium is substantiated by measurements with the unsupported foils.

In Fig. 4 are shown the results of a detailed investigation of the behavior of the narrow resonance as the target thickness was varied. When the true resonance width and the loss of energy in the target are comparable, the yield from the target must be obtained by integration of the Breit-Wigner dispersion formula over the energy interval represented by the loss in the target. We have for the yield

$$Y=\int_{E-\xi}^{E}(\sigma/\epsilon)dE, \qquad (12)$$

where ϵ is the stopping cross section for the incident particle per disintegrable nucleus in the target material and ξ is the loss of energy in the target. We assume that ϵ and ξ are independent of E over the resonance. On this assumption $\xi=nt\epsilon$, where n is the number of disintegrable nuclei per cc of the target material and t is the target thickness, and ϵ can be evaluated at the resonance energy. We also assume that σ follows the dispersion equation,[10] neglecting wave-length

[9] W. J. Hushley, Phys. Rev. **67**, 34 (1945).

[10] G. Breit and E. Wigner, Phys. Rev. **49**, 519 (1936).

and penetration factors:

$$\sigma=\sigma_R\frac{\Gamma^2/4}{(E-E_R)^2+\Gamma^2/4}, \tag{13}$$

where σ_R is the cross section at the resonance energy E_R and Γ is the full width of resonance at half-maximum intensity. Then

$$Y=\frac{\sigma_R\Gamma}{2\epsilon}\left[\tan^{-1}\frac{E-E_R}{\Gamma/2}-\tan^{-1}\frac{E-E_R-\xi}{\Gamma/2}\right]. \tag{14}$$

For a thick target ($\xi>\Gamma$) this becomes

$$Y=\frac{\sigma_R\Gamma}{2\epsilon}\left[\frac{\pi}{2}+\tan^{-1}\frac{E-E_R}{\Gamma/2}\right]. \tag{15}$$

For a given ξ, Eq. (14) has a maximum at $E=E_R+\xi/2$ given by

$$Y_{\max}(\xi)=\frac{\sigma_R\Gamma}{\epsilon}\tan^{-1}\frac{\xi}{\Gamma}. \tag{16}$$

For a thick target the maximum yield or full

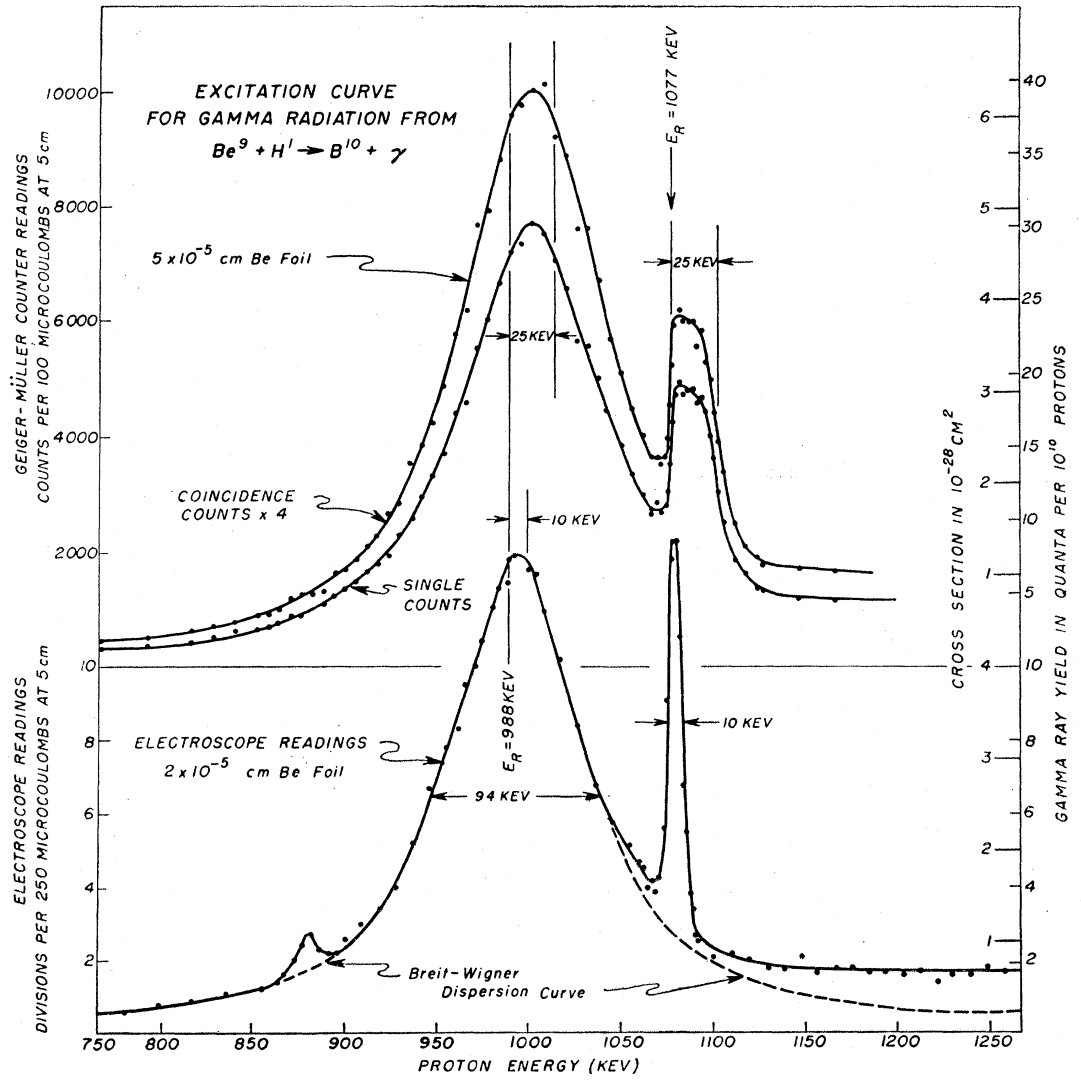

FIG. 3. Thin target excitation curves for the reaction $Be^9(p\gamma)$.

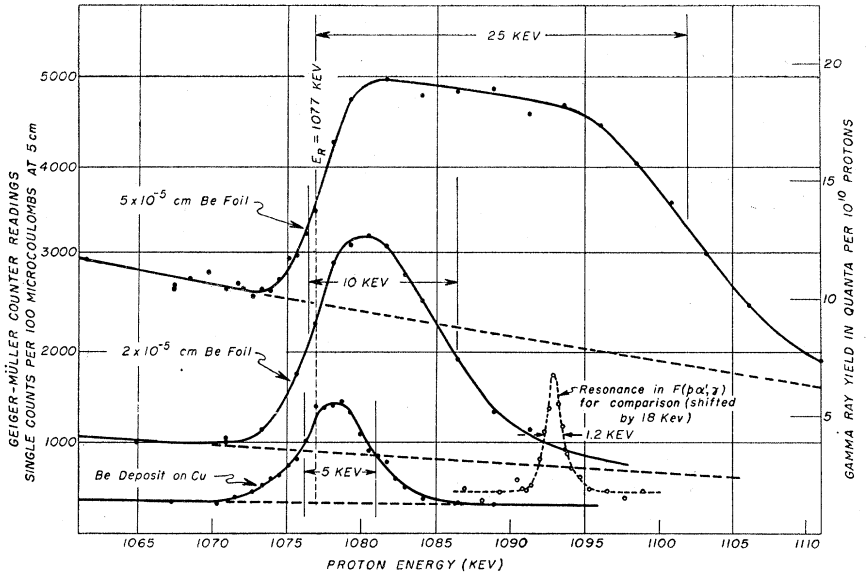

FIG. 4. Thin target excitation curves for the reaction $Be^9(p\gamma)$ in the vicinity of the 1077-kev resonance.

step in the thick target curve is

$$Y_{\max}(\infty)=\frac{\pi}{2}\frac{\sigma_R\Gamma}{\epsilon}, \tag{17}$$

so that

$$\frac{Y_{\max}(\xi)}{Y_{\max}(\infty)}=\frac{2}{\pi}\tan^{-1}\frac{\xi}{\Gamma}, \tag{18}$$

which is illustrated in Fig. 5. The function of Eq. (14) has an apparent width at half-maximum given by

$$\Gamma'=(\Gamma^2+\xi^2)^{\frac{1}{2}}, \tag{19}$$

which is also illustrated in Fig. 5.

The area under the excitation curve for a given ξ or target thickness is given by

$$A(\xi)=\int YdE=\frac{\pi}{2}\frac{\sigma_R\Gamma}{\epsilon}\xi=\xi Y_{\max}(\infty) \tag{20}$$

and is thus proportional to the loss of energy in the target and to the thick target yield above resonance. A general proof of this result has been given by Bernet *et al.*,[11] showing that it is independent of the homogeneity of the beam, the thickness of the target, and the exact nature of the thin target yield curve. It often provides a method of determining the thickness of a target by comparing its yield with that of a thick target.

From the behavior of expressions (18) and (19) we see that where ξ is large compared to Γ, the yield is approximately constant but the width varies linearly with ξ. When ξ is reduced to values comparable to Γ and lower, then the width approaches Γ while the yield varies linearly with ξ. This behavior is illustrated by the 1077-kev resonance in Fig. 4, where the excitation curves for three different targets are shown. The energy loss of the protons in the two foil targets is large compared to the true width at the narrow resonance as is indicated by the fact that they both give about the same maximum yield for this resonance, while the thinner of the two targets gives less for the radiation from the wide resonance at 988 kev which is here evidenced as a slowly decreasing background. The observed widths at the 1077-kev resonance are 10 kev and 25 kev, respectively, for the 2×10^{-5} cm and 5×10^{-5} cm targets when inclined at 35° to the beam as in these experiments. These values correspond to a stopping cross section in Be for 1-Mev protons of 3.4×10^{-15} electron volt-cm^2 and a stopping power of the Be atom relative to the air "atom" of 0.6. This is consistent with the stopping power of light elements given by Livingston and Bethe.[12]

On going to a still thinner evaporated beryl-

[11] E. J. Bernet, R. G. Herb, and D. B. Parkinson, Phys. Rev. **54**, 398 (1938).

[12] M. S. Livingston and H. A. Bethe, Rev. Mod. Phys. **9**, 245 (1937).

lium deposit on copper, both the yield and the width decrease. The area under this curve and the yield of the broad resonance indicate a target width of 3 kev, so that from the observed width of 5 kev and Eq. (7) the true resonance width is 4 kev. Alternatively the maximum yield and Eq. (6) can be employed to determine the true resonance width. The maximum yield is 40 percent of that from a thick target, so that $\xi/\Gamma=\tan 0.2\pi=0.73$. Then with $(\Gamma^2+\xi^2)^{\frac{1}{2}}=5$ kev one obtains $\xi=3$ kev and $\Gamma=4$ kev. That the width after target correction is not due to spread in beam energy is indicated by a resonance in the $F(p\alpha', \gamma)$ reaction taken at the same bombarding energy in which the total width is only 1.2 kev, thus setting an upper limit for the spread in energy of the beam (see dashed resonance, Fig. 4). The spread in beam energy is believed to be not greater than 200–300 electron volts.

The shift ($\frac{1}{2}\xi$) in the energy at which maximum intensity occurs for different target thickness is also illustrated in Fig. 4 as well as in Fig. 3. After appropriate corrections for target thickness the resonance energies are found to be 988 and 1077 kev. We neglect variations of the wavelength and barrier penetration factors over the resonance. This variation from one point of half-maximum intensity to the other is theoretically small in this case (<5 percent for the effect of both factors for the broad resonance), but we will have occasion to discuss this effect in $C^{12}(p\gamma)$ and $C^{13}(p\gamma)$ later. We conclude from these observations that the resonance at 0.988 Mev has a width of 94±5 kev, while that at 1.077 Mev has a width of 4±1 kev.

Thick target excitation curves for $Li^7(p\gamma)$, $C^{12}(p\gamma)$, $C^{13}(p\gamma)$, and $F^{19}(p\alpha', \gamma)$ have been obtained at several well-known low lying resonances (Fig. 1). Thin target curves have also been obtained for $Li^7(p\gamma)$ and $C^{12}(p\gamma)$ (Fig. 2). In the case of $C^{12}(p\gamma)$ it was found expedient to observe the positrons which result from the radioactivity of the N^{13} produced in the reaction. At each energy on the curve the target was bombarded for one half-life (10 minutes) and then the beam cut off and the activity measured for one half-life. By subtracting from each reading one-quarter of the previous reading, an appropriate correction was made for the activity built up in previous bombardments. In the case of $C^{13}(p\gamma)$ coincidence measurements were employed with 2.5 mm of aluminum between the counters. In this manner the counts resulting from the low energy radiation (2.3 Mev) from $C^{12}(p\gamma)$ were considerably reduced in number.

The thin target curve for $Li^7(p\gamma)$ indicates the unsymmetrical nature of this resonance which was first indicated in curves of Hudson *et al.*[13]

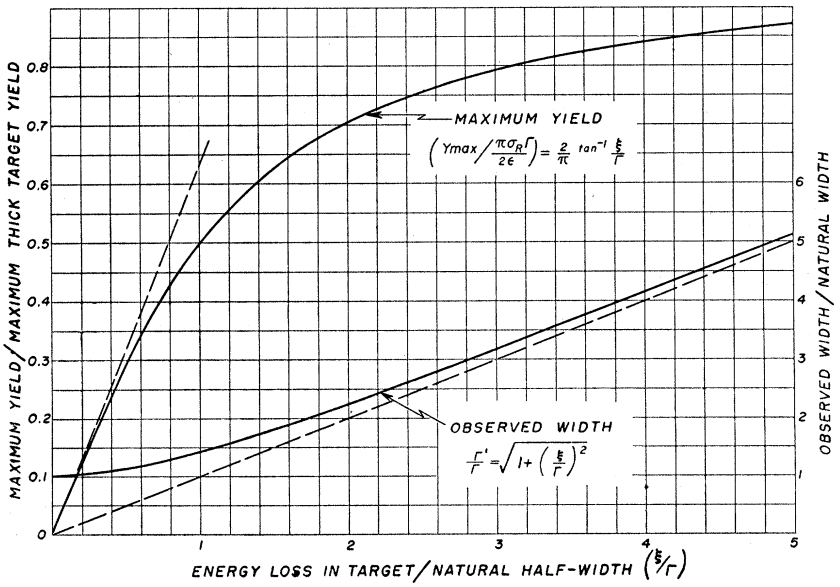

FIG. 5. The maximum yield and observed width of a resonance as a function of target thickness. The target thickness is expressed as the loss of energy of the incident particles in the target.

[13] C. M. Hudson, R. G. Herb, and G. J. Plain, Phys. Rev. **57**, 587 (1940).

TABLE I. Summary of yield and energy measurements.

Source	Resonance energy kev	Energy of radiation Mev	Range of secondaries d_7 (Al) cm	Thick target yield electroscope disintegrations/proton	Thick target yield counter disintegrations/proton	$\omega\gamma$ ev	Γ kev	σ_R cm²
$Li^7(p\gamma)$	439	17.5[a]	2.91	5.6×10^{-9}	5.1×10^{-9}	8.9	12[d]	5.7×10^{-27}
$Be^9(p\gamma)$	988	7.4	1.26	1.82×10^{-8}	1.74×10^{-8}	12.5	94	4.4×10^{-28}
	1077	6.7, 0.8	1.11	1.05×10^{-9}	0.97×10^{-9}	0.77	4	5.8×10^{-28}
$C^{12}(p\gamma)$	453	2.3[b]			7.3×10^{-10}	0.63	35	1.2×10^{-28}
$N^{13}(\beta^+)$		1.25[c]			7.2×10^{-10}			
$C^{13}(p\gamma)$	550	2.3, 5.8, 8.1			1.8×10^{-10}	15	40	2.0×10^{-27}
$F^{19}(p\alpha',\gamma)$	338	6.3		1.67×10^{-8}	1.74×10^{-8}	30	4	6.5×10^{-26}
	All $\leqslant 960$	6.3	1.06	6.80×10^{-7}	6.95×10^{-7}			

Target materials: LiOH, Be metal, Acheson graphite, CaF_2.
[a] Weak radiation near 14 Mev neglected in these calculations.
[b] Plus two annihilation quanta.
[c] Maximum energy of the positrons.
[d] Corrected for radiation observed above resonance.

Considerably more radiation is produced at bombarding energies above resonance than is to be expected from the Breit-Wigner formula. The nature of this radiation has been investigated in detail by Tangen.[14] In the excitation curves it is necessary to make a correction for this radiation, and the corrected curves are indicated by dashed lines in Figs. 1 and 2. The resonance width taken as the energy interval between the points of $\frac{1}{4}$- and $\frac{3}{4}$-maximum intensity on the corrected curve is 12 kev. Following the conventional procedure the proton energy has been taken as 440 kev at the point of $\frac{1}{2}$-maximum intensity on the uncorrected curve.[15] An error of about 1 kev is involved in designating this as the actual resonance position.

The thick target curve for the first $F(p\alpha',\gamma)$ resonance shown in Fig. 1 follows the arctangent law of Eq. (15) within the experimental errors. The variation of penetration factors over the resonance can be expected to be small, and thin target curves indicate very little yield above resonance. The resonance occurs at 338 kev, which is to be compared with the value 334 kev given by Bernet[11] *et al.* The width of the resonance is 4 ± 1 kev.

In the thin target curve for $C^{12}(p\gamma)$ a considerable asymmetry is observed. In this case, however, such asymmetry is to be expected because of the variation of the barrier penetration and wave-length factors in the Breit-Wigner formula. To show these factors we must write, instead of Eq. (13), the following:[10]

$$\sigma=\pi\lambda^2\frac{\omega\Gamma_1\Gamma_2}{(E-E_R)^2+\Gamma^2/4}, \tag{21}$$

where $2\pi\lambda$ is the wave-length of the incident proton in the center of mass system, ω is a statistical weight factor of the order of unity, Γ_1 is the width for re-emission of the incident particle, and Γ_2 is the width for the decay of the compound nucleus by the first stage of the process under observation. If one is observing gamma-radiation from a compound nucleus produced by proton bombardment $\Gamma_1=\Gamma_p$ and $\Gamma_2=\Gamma_\gamma$. If the radiation is given off by a residual nucleus produced in alpha-particle emission by proton bombardment, $\Gamma_1=\Gamma_p$ and $\Gamma_2=\Gamma_{\alpha'}$. In either case Γ_2 is not sensitive to the bombarding energy, since the gamma-ray or short range alpha-energy changes only by relatively small fraction over the resonance. On the other hand, the proton width, Γ_p, varies considerably over a wide resonance when the particle energies are small compared to the height of the potential barrier. In the bombardment of C^{12} and C^{13} by protons the resonances occur near 0.5 Mev, considerably below the top of the potential barrier ($\sim$2 Mev), and are approximately 40 kev wide. In the $Be(p\gamma)$ case the broad resonance near 1 Mev is close to the top of the barrier ($\sim$1.5 Mev), while in the $Li(p\gamma)$ and $F^{19}(p\alpha',\gamma)$ cases the resonances are relatively narrow.

When Γ_p does not vary appreciably over the resonance, the resonance energy is that point at which the thick target yield has reached one-half

[14] R. Tangen (in publication).
[15] L. R. Hafstad, N. P. Heydenburg, and M. A. Tuve, Phys. Rev. **50**, 504 (1936).

its maximum value, and the resonance width is the energy interval between the points at which the yield is one-quarter and three-quarters of its maximum value. Small corrections are necessary when Γ_p does vary appreciably over the resonance, and we have made such corrections in the cases of $C^{12}(p\gamma)$ and $C^{13}(p\gamma)$. The final results for all resonance positions and widths reported here are tabulated in Table I.

5. ENERGY OF THE GAMMA-RADIATION

Early measurements of the energy of the gamma-radiation produced in the disintegration of light nuclei were made by two methods:

1. Determination of the absorption coefficient of the radiation.

2. Determination with a magnetic field of the momentum (and thus of the energy) of the secondary Compton electrons and pairs produced in a thin lamina placed across a Wilson cloud chamber.

Neither of these methods is ideal, and in recent measurements emphasis has been placed on two alternative methods:

3. Coincidence counter measurements of the range of the secondaries.

4. Beta-ray spectrometer measurements of the energy of the secondaries.

a. Absorption Coefficient Measurements

For radiation below 1 Mev the absorption of radiation is largely due to the photoelectric effect in elements of large Z, and the absorption coefficient is a rapidly decreasing function with energy. Method 1 can be employed with considerable success in this region. By direct comparison with the absorption of annihilation radiation the energy can be found with some accuracy, as in the case of the 480-kev radiation[13,16] from the low lying excited state of Li^7. For higher energies the photo-effect becomes negligible, aad the absorption is due to the Compton effect (σ_c) and pair formation (σ_p). For energies from 2 to 20 Mev the absorption coefficients per electron or electronic cross sections†††† are given approximately by[17]

$$\sigma_c = \pi r_0^2 \frac{mc^2}{h\nu} \ln 1.2 \frac{h\nu}{mc^2}, \tag{22}$$

$$\sigma_p = \pi r_0^2 \frac{Z}{165} \ln \frac{h\nu}{4.3mc^2}, \tag{23}$$

where r_0 is the "classical" electron radius. The total cross section, $\sigma = \sigma_c + \sigma_p$, thus decreases to a minimum in the region from 3 to 10 Mev, depending on Z and then rises again. The minimum point occurs at $h\nu_m$ given by

$$\frac{mc^2}{h\nu_m} \ln \frac{h\nu_m}{2.3mc^2} = \frac{Z}{165}, \tag{24}$$

but it must be emphasized that the minimum is a very broad one. By the use of absorbers of different Z the ambiguity arising from the fact that a given absorption coefficient holds for two energies can be avoided.

Actually, in absorption measurements with "poor" geometry where the radiation scattered in the Compton effect, the radiation from pair annihilation, and the bremsstrahlung from the secondary electrons are not excluded from the detector, the absorption coefficient measured is closer to that calculated from the true energy absorption by the electrons.[18] This is given by

$${}_a\sigma' = \eta_a\sigma = \eta({}_a\sigma_c + {}_a\sigma_p), \tag{25}$$

where

$$\eta = 1 - \frac{Zh\nu}{5000mc^2}$$

is the "bremsstrahlung" term,

$${}_a\sigma_c = \pi r_0^2 \frac{mc^2}{h\nu} \ln \frac{h\nu}{1.1mc^2}$$

is the cross section for energy transfer to the electron by the Compton effect, and

$${}_a\sigma_p = \frac{h\nu - 2mc^2}{h\nu} \sigma_p$$

[16] L. H. Rumbaugh, R. B. Roberts, and L. R. Hafstad, Phys. Rev. **54**, 657 (1938); S. Rubin, Phys. Rev. **69**, 134A (1946); K. Siegbahn, Ark. f. Ast. Math. Fyz. **34B**, No. 6 (1946); Lauritsen, Fowler, Lauritsen, and Rasmussen, Phys. Rev. **73**, 636 (1948).

†††† For convenience we employ electronic cross sections even though σ_p arises from an interaction with the nuclear field. Multiplication by the number of electrons per cc yields the absorption coefficients per cm.

[17] W. Heitler, *The Quantum Theory of Radiation* (Oxford University Press, London, 1935).

[18] J. F. Streib, W. A. Fowler, and C. C. Lauritsen, Phys. Rev. **59**, 253 (1941).

is the pair formation cross section corrected for the eventual annihilation of the positron member.

The equilibrium with the secondary ionizing and non-ionizing radiations is reached relatively quickly, as is illustrated in calculations made for 17.5-Mev radiation by Delsasso, Fowler, and Lauritsen.[19] The actual absorption coefficient measured will depend, of course, on the relative sensitivity of the detector to the primary and secondary radiations but not very critically. More important is the fact that the scattered radiation has an absorption coefficient smaller than that for the primary radiation if the primary energy is greater than $h\nu_m$. The practical result is that in absorbers of high Z, such as lead, the observed coefficient is about equal to that at the minimum in the curve, namely, 14×10^{-24} cm^2 per Pb atom or 0.46 per cm of Pb for all gamma-energies from 2 to 17.5 Mev. Even for absorbers of low Z such as Al, the coefficient varies by less than 50 percent over this region. By using a cloud chamber as detector, Delsasso, Fowler, and Lauritsen[19] were able to exclude the effects of secondary gamma-radiation and found an absorption coefficient of 0.66 per cm for 17.5-Mev radiation which is 90 percent of the theoretical value of 0.73 per cm. Using the same arrangement, a value of 0.44 per cm for 6.3-Mev radiation was obtained, the theoretical value being 0.5 per cm. It is clear from these considerations that the method is not satisfactory for critical determination of quantum energies of energies above 2 Mev.

b. Cloud-Chamber Measurements

Cloud-chamber measurements of the momentum of secondaries produced by gamma-rays are also subject to serious defects. These arise primarily from the necessity of determining accurately the "history" of the secondary. The fraction of the quantum energy given to the secondary must be known, and the amount of energy it has lost in traversing matter before observation in the cloud chamber must be known. In regard to the latter point it is necessary that the secondaries be produced in a thin lamina in which they lose little energy. The lamina must be placed in the chamber so that observations of particles is possible on the side near the source as well as away from it. The beam must be collimated so that only the lamina and not the chamber walls and top are radiated. A thin window should be mounted in the wall between lamina and source. There is the further complication that Compton electrons receive considerably less than the full quantum energy when ejected at an angle with the gamma-radiation.

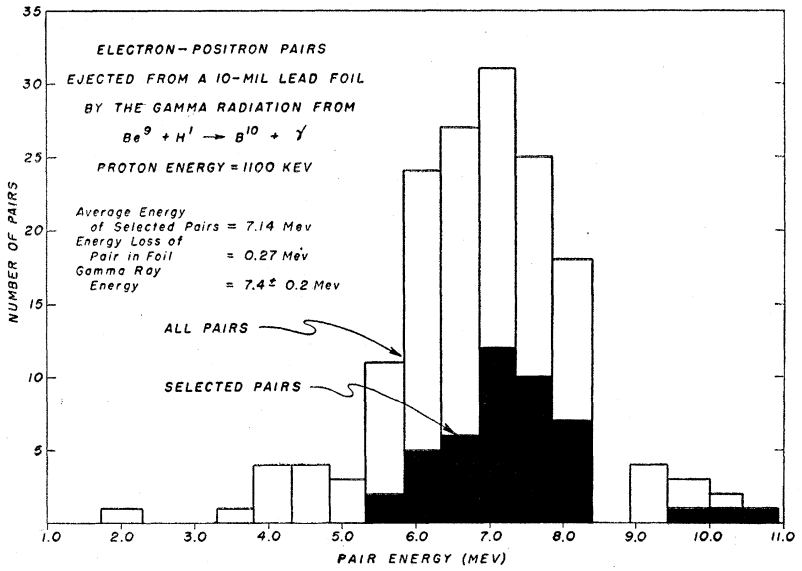

FIG. 6. Electron-positron pairs ejected from a 0.010-in. lead foil by the gamma-radiation from $Be^9(p\gamma)$.

[19] L. A. Delsasso, W. A. Fowler, and C. C. Lauritsen, Phys. Rev. **51**, 391 (1937).

The fractional energy received is given by

$$\frac{E_0}{h\nu} \approx 1 - \frac{mc^2}{2h\nu} - \theta^2 \frac{h\nu}{2mc^2}, \tag{26}$$

when θ, the angle of ejection, is small. We note that for high energy radiation the dependence of E_0 on θ is critical. It is true that small angles of ejection and thus large energy transfers are most probable, but the complication still exists. In addition, because the Compton effect decreases with energy, radiation scattered by the cloud-chamber structure and the field producing coils will produce secondary electrons in the lamina more frequently than will the higher energy primary radiation. These electrons will, of course, usually make large angles with the direction of the unscattered beam. We have found that the least ambiguity is involved in the use of pairs rather than the Compton electrons. If the intensity of the source is adjusted to give relatively few secondaries per cloud-chamber expansion, there is no difficulty in recognizing the existence of the pairs and of ascertaining definitely whether they originate in the thin lamina. The full energy of the quantum appears in the kinetic and mass energy of the two pair members. Low energy scattered radiation has a smaller probability of producing pairs than the primary radiation, and the resultant of the momentum vectors of the pair members must pass through the source if the pair is due to the primary radiation. The main objection to the use of pairs arises from the fact that low energy components in the primary radiation produce relatively few pairs and are thus difficult to detect unless they are of high intensity. In addition, there is a major difficulty in cloud-chamber measurements in that the method is tedious and time consuming both in obtaining the cloud-chamber photographs and in analyzing them. Furthermore, errors arise in the measurement of the radii of curvature of the tracks resulting from spurious curvature caused by the scattering in the gas. An energy resolution of about 1 Mev is the best that can be obtained in practice.

Nevertheless, we have employed the method in the determination of several gamma-ray energies. The results are tabulated in Table I where the original determinations have been corrected for new field coil calibrations. The radiation from F^{19} bombarded by protons has also been studied by Phillips and Kruger,[20] who measured the energies of pairs produced in the cloud-chamber gas by the radiation. They have found a number of lines, whereas we have found only one at 6.3 Mev. At the high bombarding energies employed by them additional gamma-ray components may appear.

The most recent measurements have been made in the Be($p\gamma$) reaction. The energy distribution of the pairs observed in a 0.25-mm lead lamina is shown in Fig. 6. The superior resolution of selected pairs on which the most accurate curvature measurements could be made is evident. These have an average kinetic plus mass energy of 7.1 Mev with a spread at half-maximum intensity of 2 Mev. Correction for the loss of energy in the foil by the pairs yields 7.4 ± 0.2 Mev for the quantum energy where the error given is the statistical error calculated by dividing the root mean square deviation in energy by the square root of the number of pairs.

c. Coincidence Counter Measurements

Coincidence counter measurements of the range of the secondaries produced by gamma-rays have been very useful in the energy range from 0.1 to 3 Mev, and a very general treatment of the subject has been recently given by Bradt *et al.*,[21] and by Bleuler and Zünti.[22] One of the earliest measurements of high energy radiation by this method was Bothe's measurements[23] of the gamma-radiation from beryllium and boron bombarded by alpha-particles. This method has also been applied at high energies by Curran, Dee, and Petržílka,[2] Hushley,[9] and Bennett *et al.*[24] We will follow the discussion of Bleuler and Zünti in discussing the application to high energy gamma-rays. The extension to higher energies is straightforward when pair formation and radiation are taken into account.

The coincidence counter arrangement has been

[20] J. A. Phillips and P. G. Kruger, Phys. Rev. **72**, 164 (1947).
[21] H. Bradt, P. C. Gugelot, O. Huber, H. Medicus, P. Preiswerk, and P. Scherrer, Helv. Phys. Acta **19**, 77 (1946).
[22] E. Bleuler and W. Zünti, Helv. Phys. Acta **19**, 376 (1946).
[23] W. Bothe, Zeits. f. Physik **59**, 1 (1929).
[24] W. E. Bennett, T. W. Bonner, and B. E. Watt, Phys. Rev. **59**, 793 (1941).

described in Section 3b. Secondary electrons and pairs produced in the converter by the incident gamma-rays pass through two counters or two sets of counters in which coincidences can be measured. The absorption is measured by inserting layers of absorber between the counters. In such an arrangement when counter and absorber are of the same material the ratio of the number of coincidence counts with absorber to the number with no absorber is given by

$$\frac{N}{N_0}=\frac{\int_0^{E_{\max}}\int_d^{d+c} f(h\nu, E_0)p(E_0, x)dE_0dx}{\int_0^{E_{\max}}\int_0^{c} f(h\nu, E_0)p(E_0, x)dE_0dx}. \quad (27)$$

In this expression $f(h\nu, E_0)dE_0$ is the probability for the production of a secondary of energy E_0 by a quantum of energy $h\nu$, and $E_{\max}$ is the maximum energy of the secondaries. The term $p(E_0, x)dx$ is the probability that an electron or a positron of energy E_0 will penetrate a thickness x of the material used as converter and absorber. The converter and absorber thicknesses are c and d, respectively. A "thick" converter, i.e., one for which c is greater than the maximum range of the secondaries, is customarily used in coincidence measurements.

In omitting any dependence of $f(h\nu, E_0)$ on the angle of ejection of the secondary we assume, as is usually the case, that the possible angular divergence of the secondaries through the coincidence counters is large enough to permit all secondaries to contribute to the counting regardless of their angle of ejection with the direction of the incident quanta. The angular divergence in the arrangements we employed was $\pm 45°$ in the plane normal to the counter axes and $\pm 80°$ in the plane of the counters. For radiation above several Mev the kinetic energy of an electron ejected in the Compton effect at an angle θ with the incident quantum is given by

$$E_0=2mc^2\cot^2\theta \quad (28)$$

for not too small θ. We thus note that all electrons with more than 1-Mev energy are ejected within a cone of half-angle 45°.

It is often convenient to employ the forward counter as a monitor as d is varied. In case N_0 in Eq. (27) is taken as the number of counts in the forward counter, an additional solid angle factor which may be a function of $h\nu$ but not of d must be included.

We have neglected all geometrical factors in expressing $p(E_0, x)$ as a function only of E_0 and x. The actual behavior will be discussed in connection with the experiments designed to test the dependence of the measurements on geometrical factors. We note that N is fundamentally dependent on the probability of penetration for electrons of homogeneous energy appropriate to the geometry of the experiment. To obtain N/N_0 this probability must first be averaged over the total thickness of converter and absorber and then over all possible secondary energies weighted by their probability of occurrence.

The function $p(E_0, x)$ for homogeneous electrons has been discussed by Bleuler and Zünti for energies up to 3 Mev and will be derived approximately for energies up to 17.5 Mev in Section 6f. For small x it decreases as the electrons are scattered from the beam, and is in this region very sensitive to the geometry of detection. As x increases the electron energy becomes smaller because of loss by ionization, and the scattering becomes so large that "diffusion" sets in. The particles are stopped by the combination of scattering and energy loss, and absorption as well as scattering must be taken into account. While at high energies (small x) the electrons can also radiate, and since this is accompanied by large energy losses it can be treated as a mechanism of absorption rather than a gradual energy loss. Neither the radiative nor the diffuse absorption is particularly sensitive to geometry.

For a given converter thickness N/N_0 is measured as a function of d. From the observed curve two absorber thicknesses are usually determined. In Bleuler and Zünti's notation these are d_1, the thickness in which N/N_0 has decreased to 2^{-1} and d_∞, the thickness in which N/N_0 has decreased to zero. The half-value layer d_1 is, of course, dependent in a very complicated manner on the composition of the radiation as well as its maximum energy. The cut-off thickness, d_∞, is very difficult to determine because of the existence of background, accidental counts, and the fact that the tail of the N/N_0 curve makes a high

order contact with the d axis. Because of these difficulties, Bleuler and Zünti have made semi-empirical determinations of the d_n values corresponding to values of $N/N_0=2^{-n}$ for n up to 7 for 0.5-, 1.5-, and 2.62-Mev radiation and in addition have given direct experimental values for a few d_n's for 6.3- and 17.5-Mev radiation.

In connection with calibrations of this method we have similarly determined d_n for 2.62-, 6.3-, and 17.5-Mev radiation and have investigated the dependence on geometrical arrangements. In order to obtain maximum intensity the separations between target and forward counter and between forward counter and rear counter are kept to a minimum and are usually made only slightly larger than the maximum converter and absorber thicknesses to be employed. These are just equal to the range of the highest energy secondaries in the converter and absorber material. In such an arrangement we have also used two counters in parallel in the rear position, so that in the plane of the minimum angles (normal to the counter axes) they subtended the same angle at the target as the forward counter. This would be equivalent to "poor" geometry in gamma-ray absorption measurements. It must be recalled, however, that in gamma-ray absorption measurements one is anxious to exclude from the detector the degraded, scattered radiation produced in the absorber if one desires to measure the true attenuation coefficient which is more critically dependent upon energy than the energy absorption coefficient. In measurements on the secondary electrons, however, one attempts essentially to measure the "range" of these particles. It is then desirable to detect them as effectively as possible, even though scattered, until they are actually stopped in the absorber. If the possible angular divergence of path through the coincidence arrangement from the converter is larger than the mean scattering angle, the nearest approach to a true "range" behavior will be reached.

Because of the need for high intensity these considerations are somewhat academic except in one regard. With the separations described above set for the maximum converter and absorber thicknesses, the position of thin converters or absorbers is still arbitrary. In Fig. 7 are shown the results of absorption measurements with a thick converter on the radiation from $Li^7(p\gamma)$ at 440 kev, in one case with the first absorbing

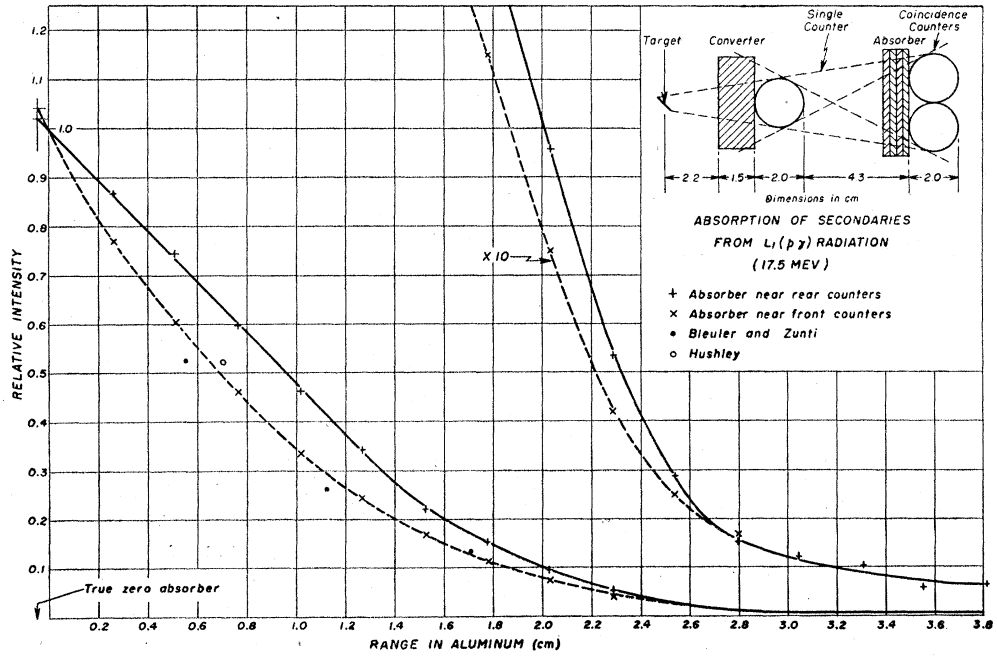

FIG. 7. Absorption of the secondaries produced in a thick aluminum converter by the $Li^7(p\gamma)$ radiation (17.5 Mev).

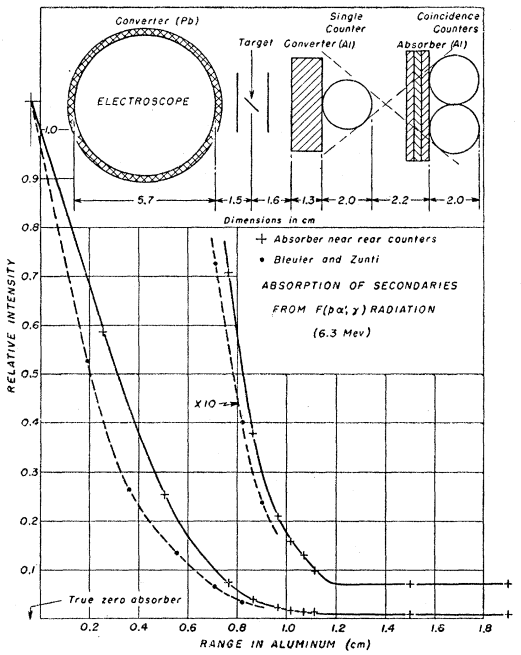

FIG. 8. Absorption of the secondaries produced in a thick aluminum converter by the $F^{19}(p\alpha', \gamma)$ radiation (6.3 Mev).

layer placed just behind the forward counter and successive layers placed immediately behind it and in the other case with the first absorbing layer placed just before the rear counters and so on. It will be noted that the second alternative gives a flatter curve, the half-value layer being 9.6 mm while in the first case it is 6.6 mm. For large absorber thicknesses the curves, of course, come together. Bleuler and Zünti give 5.8 mm for an arrangement, using only one rear counter and absorbers near the forward counter. This dependence of the absorption curves on the position of the first few absorbers can be readily understood on the basis that scattering will remove particles from the secondary beam when the absorber is some distance from the rear counter while it will not do so as effectively when the absorber is placed up against the rear counters. We have preferred the second alternative, especially in investigations of composite radiation, feeling it desirable to have as large as possible a reading due to hard components when the softer components are completely absorbed. The main point of interest, however, is the fact that the half-value and other intermediate layers are very sensitive to the geometrical arrangement even for homogeneous radiation.

We have not found the absorption curves to be as critical to the position of thin converters. This is in part because of the fact that "zero" converter cannot be obtained in practice because of target supports, shields, and other materials which produce secondaries. Most of the results were obtained with thick converters. In general, we placed the converters near the forward counter rather than the target in order to minimize the coincidence counts resulting from the low energy secondaries produced at large angles with the direction of the quanta. In this way flatter curves were obtained. This arrangement did, of course, increase the ratio of the number of single counts for all absorber thicknesses.

An important parameter of any experimental arrangement is the ratio of coincidence counts to single counts for no absorber and a thick converter. In the arrangement we have used with two rear counters and one single counter this ratio would be ~ 0.6 if the secondaries were ejected only in the direction of the quanta and were not scattered in the converter. We actually find the ratio to be $\frac{1}{3}$ for 6.3-Mev radiation from $F(p\alpha, \gamma)$ and for 17.5-Mev radiation from $Li(p\gamma)$ and $\frac{1}{4}$ for 2.6-Mev radiation from ThC″ filtered by $\frac{1}{8}$ in. brass. Allowance has been made for the absorption in the counter walls by extrapolation to true zero absorbers. Since the ThC″ ratio is low because of softer components, it is clear that for hard radiation from 2.6 to 17.5 Mev the ratio is approximately constant. This means that for hard radiation, at least, the effect of the angular distribution of the secondaries and of the scattering in the converter has been minimized by the use of large angles of detection in the coincidence arrangement. For small values of this ratio it will not be independent of energy nor will the shape of the absorption curve be independent of this factor. It is suggested that this ratio should always be stated in giving the results of absorption measurements.

Absorption curves for the secondaries produced in thick aluminum converters by the radiation from $Li^7(p\gamma)$, $F(p\alpha', \gamma)$, and ThC″ are shown in Figs. 7, 8, and 9. From these curves we have determined d_1 to d_8, values for which are tabu-

lated in Table II and shown graphically in Fig. 10. In Fig. 10 we also show d_∞, the maximum theoretical range of the maximum energy secondaries which can be produced by the gamma-radiation and $\bar{r}(h\nu)$, the average range of secondaries produced in a thin layer of the converter. The average range of the secondaries produced in a thick converter, $\bar{d}(h\nu)$ is not shown but is approximately equal to $1.1d$. For high energy radiation, the maximum energy of the secondaries is $h\nu - \frac{1}{2}mc^2$, or 255 kev less than the quantum energy, $h\nu$. The calculation of the maximum and average range is discussed in Section 6c. In the notation employed there, we will have $d_\infty = R(h\nu - \frac{1}{2}mc^2)$.

By means of the coincident counter arrangement used in the $F(p\alpha', \gamma)$ investigation, we have made a detailed study of the energy of the radiation emitted at the 0.988- and 1.077-Mev resonances in the disintegration of beryllium by protons. Early investigations[2, 9] have shown that the energy of the radiation is such as to indicate that it originates from the compound nucleus B^{10}. Curran[2] *et al.*, showed that the maximum gamma-ray energy corresponded to the energy balance in the reaction and that it varied correctly with the incident energy of the protons. In addition at a bombarding energy of 1.04 Mev, Hushley[9] found that the gamma-ray energy was 7.5 Mev in good agreement with the expected value (6.5+9/10×1.04 Mev). Our own cloud-chamber measurements yielded 7.4±0.2 Mev at 1.06-Mev bombarding energy.

In these measurements we have employed aluminum absorbers and aluminum converters. The absorption of the secondaries is shown in Fig. 11. In this curve the number of coincidence counts relative to the single counts in the counter nearest the target is plotted as a function of the thickness of absorber between the counters. The "zero" absorber arising from the two counter walls (30 mg/cm² per wall) corresponds to about 0.33 mm of aluminum. These curves were obtained with a 12.7-mm Al converter. It is clear from the figure that the maximum energies of the radiations at the two resonance energies are approximately equal but that the curves are not identical at all points. For transitions to the ground state of B^{10} one would expect the maximum energy radiation from the 1.077-Mev resonance to be 79 kev greater in energy than that from the 0.988-Mev resonance. This difference would not have been detectable. From Fig. 3 we note that the radiation at a bombarding energy of 1.077 Mev consists in part of the radiation from the broad 0.988-Mev resonance, and the 1.077-Mev curve has been corrected as shown in Fig. 11. We then see that the end pot infor the 1.077 Mev resonance is definitely less than at 0.988 Mev, as indicated in the end portion of the curves with ordinates multiplied by 10. A comparison with the 6.3-Mev gamma-ray from the

TABLE II. Range of secondary electrons in aluminum (cm) (thick aluminum converter).

Thickness	Relative intensity	Energy of radiation: 2.6 Mev a	2.6 Mev c	6.3 Mev a	6.3 Mev c	17.5 Mev a	17.5 Mev b	17.5 Mev c
d_1	0.5000	0.118	0.09	0.37	0.22	0.96	0.66	0.58
d_2	0.2500	0.178	0.165	0.52	0.41	1.46	1.23	1.16
d_3	0.1250	0.223	0.225	0.68	0.59	1.88	1.70	1.74
d_4	0.0625	0.268	0.27	0.79	0.74	2.22	2.09	—
d_5	0.0312	0.298	0.31	0.88	0.85	2.47	2.38	—
d_6	0.0156	0.343	0.34	0.98	0.93	2.66	2.63	—
d_7	0.0078	0.383	0.37	1.06	—	2.91	2.91	—
d_8	0.0039	0.408	—	1.13	—	3.18	3.18	—
d_∞ (calc.)	0	0.50	0.44	1.34	—	3.59	3.59	—

a = absorber near front counter.
b = absorber near rear counter.
c = results of Bleuler and Zünti.

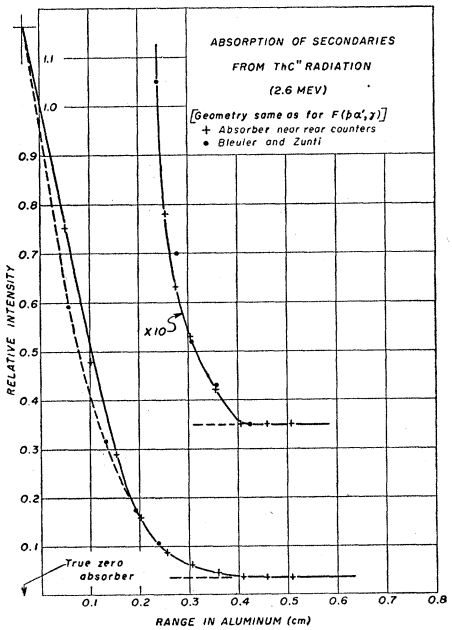

FIG. 9. Absorption of the secondaries produced in a thick aluminum converter by ThC" radiation (source surrounded by 3 mm of brass). See Fig. 8 for the geometry of the counter arrangement.

$F^{19}(p\alpha', \gamma)$ reaction is shown. We find the end point (actually the point at 2^{-7} or 0.8 percent of the initial intensity) of the secondaries from the 0.988-Mev and the 1.077-Mev resonances to be, respectively, 2.0±0.3 mm and 0.7±0.4 mm greater than that for the secondaries produced by the 6.3-Mev gamma-ray. The probable errors are indicative of the scatter in results obtained from several curves similar to Fig. 11. The maximum gamma-ray energies are thus 7.4±0.2 and 6.7±0.3 Mev, employing a linear range-energy relation with slope of 0.57 Mev/mm as indicated in Fig. 10 for d_7. All of the coincidence counts at 1.077 Mev beyond 12 mm of absorber can be attributed to the broad resonance at 0.988 Mev and need not be attributed to the 1.077-Mev resonance. Absorption curves taken just above and below this resonance coincide with that at 0.988 Mev.

Our value for the maximum energy of the radiation from the 0.988 resonance is about the same as that found by Hushley,[9] who measured the energy at 1.04 Mev just below the 1.077-Mev resonance. This substantiates the belief that the gamma-ray arises in a transition from the compound state in B^{10}, in which the proton is captured, to the ground state of B^{10}. The lower value for the radiation from the 1.077-Mev resonance indicates that at least a double transition is involved in the radiation to the ground state of B^{10}. The total energy of the soft component or components can be calculated from the observed energy difference of the two high energy

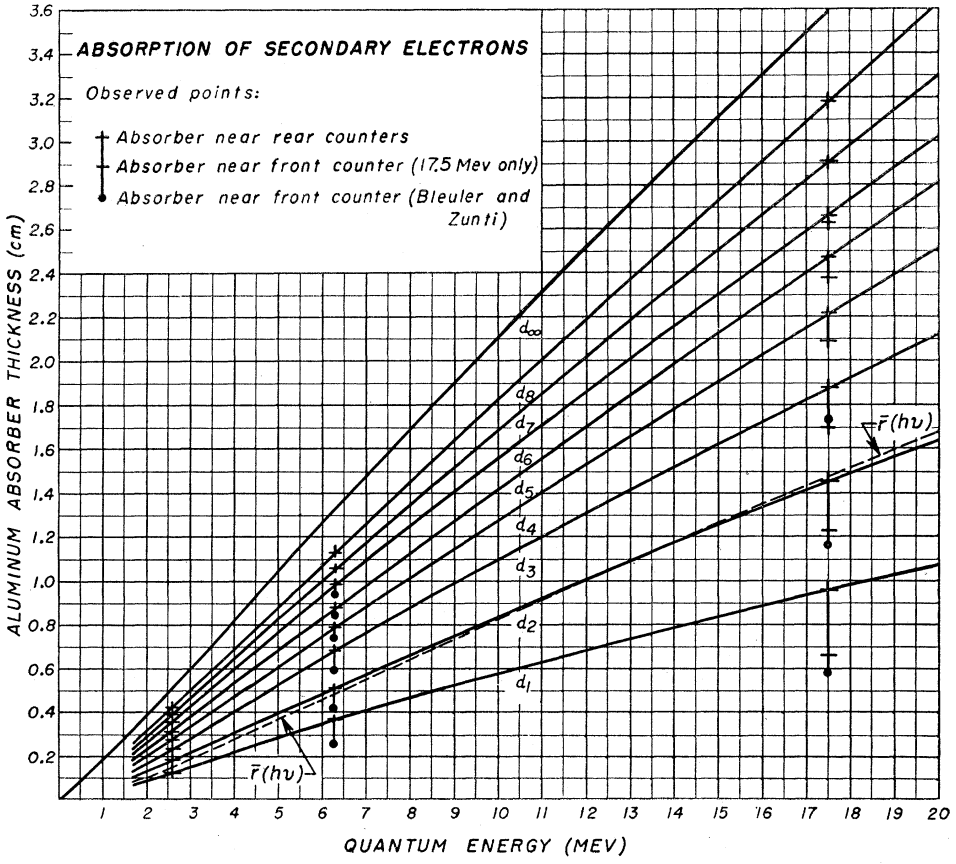

FIG. 10. The absorption of secondary electrons produced in a thick aluminum converter by gamma-radiation as determined by coincidence counter measurements. The absorber thickness which reduces the number of coincidence counts to 2^{-n} of the number without absorber is indicated by d_n. Calculated values are plotted for d_∞, the maximum range of the maximum energy secondaries produced by the gamma-radiation, and for $\bar{r}(h\nu)$, the average range of the secondaries produced in a *thin* layer of the converter. The average range of the secondaries produced in a "thick" converter, $\bar{d}(h\nu)$, is not plotted but is approximately equal to $1.1d_1$.

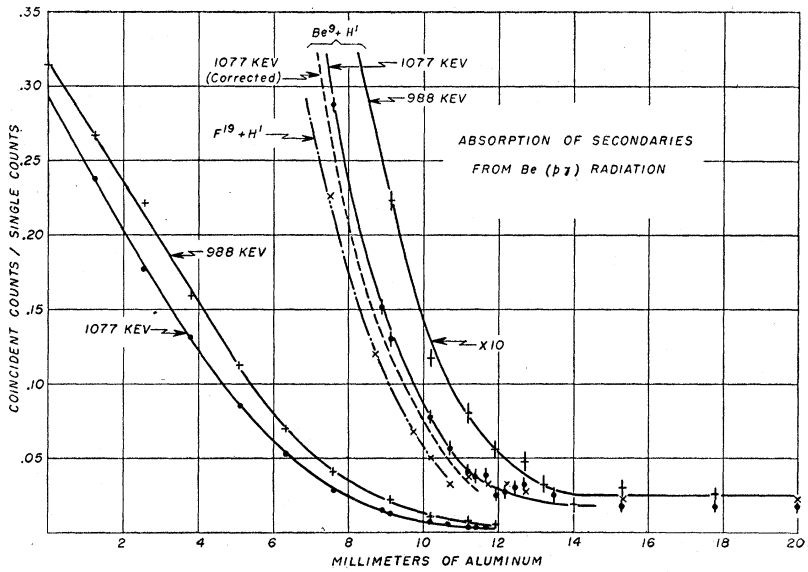

FIG. 11. Absorption of the secondaries produced in a thick aluminum converter by the $Be^9(p\gamma)$ radiation. See Fig. 8 for the geometry of the counter arrangement.

gamma-rays and from the difference in bombarding energies to be 0.8 ± 0.3 Mev. If a single intermediate level in B^{10} is involved, it is located either at 6.7 or 0.8 Mev above the ground state. There is some evidence from the yield at 1.077 Mev that the initial decay rate of this state corresponds to the primary emission of 6.7- rather than 0.8-Mev radiation. Furthermore, there is some evidence[25] for a low lying state at 0.715 ± 0.010 Mev in B^{10}. This is probably the intermediate state involved.

Direct evidence for the existence of the soft component is difficult to obtain because of the presence of the 6.7-Mev quanta in equal numbers and of some additional 7.4-Mev quanta from the broad resonance. The high energy quanta are much more efficient in producing secondaries even in the thinnest converters, namely, the counter wall and the target tube. The shielding material around the target and counters also served as converter. The absorber curves do show some evidence for a soft component in the coincidence-single count ratios at the minimum absorber, namely, the two counter walls. For high energy quanta the ratio of coincidence to single counts at the minimum absorber is approximately independent of the gamma-ray energy as discussed above. It will be noted that this is the case for the 6.3-Mev radiation from $F(p\alpha', \gamma)$ and for the 7.4-Mev radiation from the 0.988-Mev resonance. However, the 6.7-Mev quanta are presumably accompanied by soft radiation which will produce secondaries that give single counts but few coincidence counts. The minimum absorber coincidence single count ratio should just be reduced in proportion to the relative number of secondaries from the soft radiation. The 8 percent lower value for this ratio observed at the 1.077-Mev resonance seems reasonable. In order to investigate this point more closely we employed two bell-shaped counters, with adjacent 3 mg/cm² end walls, in coincidence. With these counters the ratios with no additional absorber differed by only 4 percent at the two resonances. With an additional 0.25-mm Al between counters the difference again became 8 percent. We conclude that the soft component can produce secondaries which traverse 6 mg/cm² but not 60 mg/cm² of material. This sets an upper limit of 0.6 ± 0.2 Mev for the soft quantum energy. This is in only fair agreement with the value 0.8 ± 0.3 Mev found from the difference in energies of the hard quanta.

We conclude from these measurements that the excited state in B^{10} indicated by the 0.988-Mev resonance in the $Be(p\gamma)$ reaction decays by the emission of 7.4-Mev quanta to the ground state of B^{10}. In the decay of the state indicated

[25] H. H. Staub and W. E. Stephens, Phys. Rev. **55**, 131 (1939); Lauritsen, Fowler, Lauritsen, and Rasmussen, Phys. Rev. **73**, 636 (1948).

by the 1.077-Mev resonance, 6.7-Mev quanta are involved, and there is evidence for an equal number of quanta of energy between 0.5 and 1.0 Mev.

d. Beta-Ray Spectrometer Measurements

The methods of gamma-ray energy measurement previously described are by no means ideal. The recent beautiful measurements for energies below 4 Mev by Siegbahn,[26] Latyshev,[1] and Deutsch *et al.*,[27] by means of beta-ray spectrometers of various types indicate that this method should have many advantages in the high energy region over the methods already employed in this region. A spectrometer for the study of secondaries from high energy quanta is now under construction in this laboratory. A spectrometer for secondaries below 1.5 Mev is in operation. To date one of the beta-ray spectrometer measurements which we have undertaken is a preliminary measurement of the low energy component in the radiation from the 1.077-Mev resonance in Be$(p\gamma)$. This measurement reveals a soft component at 0.72 Mev. The coincident counter measurements described above are not as accurate as this determination.

6. THE YIELD OF GAMMA-RADIATION

The yield in disintegrations per incident particle of a nuclear reaction resulting in gamma-radiation can be determined from counter or electroscope readings obtained under known conditions. In order to calculate the yield from the readings it is necessary to know, among other things, the efficiency of production of ionizing secondaries in the walls of the detecting device by the gamma-radiation. In the first part of this section we will primarily be concerned with the calculation of this factor as a function of the energy of the radiation. The quantities essentially involved are ϵ, the number of counts per incident quantum for the counter, and i, the ion pairs per unit volume per quantum per cm^2 of incident radiation for the electroscope. We will also discuss the absorption of the primary radiation in the wall material in which the ionizing secondaries are produced and the building up of secondary gamma-radiation. With a knowledge of these factors and with the experimental determination of the solid angle subtended by the detector at the source and of the angular distribution of the radiation it is possible to translate the detector readings for a given number of incident particles into the yield in disintegrations per incident particle. The results of yield measurements in several reactions will be discussed.

Empirical curves for the efficiency in counts per incident quantum for cylindrical counters‡ employing aluminum converters have been given for radiation up to 3 Mev in energy by Bradt *et al.*,[21] by Dunworth,[28] and by Deutsch.[29] Theoretical calculations have been made by v. Droste,[30] Yukawa and Sakata,[31] and by Bleuler and Zünti.[22] The latter have obtained good agreement with the experimental results of Bradt *et al.* They have essentially integrated the range of the secondaries in the medium multiplied by a factor which varies slowly with the energy of the secondary over the cross section for the production of secondaries of given energy and range. The slowly varying factor is a measure of the probability that a secondary produced in the medium can reach the counter averaged over the secondary range. This factor is less than unity because of scattering and radiative loss.

In this section we propose to extend the calculations of Bleuler and Zünti on counter efficiency to higher energy radiation and to compare the results with similar calculations on electroscopes. The results of experiments in which aluminum- and lead-lined counters and electroscopes have been employed simultaneously in yield measurements will be also discussed. The calculations will deal primarily with aluminum converters, and the experimental data on lead converters will give empirical conversion factors from lead-lined to aluminum-lined detectors.

[26] K. Siegbahn, Ark. f. Mat. Astr. o. Fys. Bd **30A**, No. 1 (1943).
[27] M. Deutsch, L. G. Elliott, and R. O. Evans, Rev. Sci. Inst. **15**, 178 (1944).

‡ This quantum efficiency for counters should not be confused with that which gives the number of counts per traversal of the counter by secondary electrons or positrons. The latter is usually about 98 percent and of course a correction must be made for it in yield determinations.

[28] J. V. Dunworth, Rev. Sci. Inst. **11**, 167 (1940).
[29] A. Roberts, J. R. Dunning, and M. Deutsch, Phys. Rev. **60**, 544 (1941).
[30] G. v. Droste, Zeits. f. Physik **100**, 529 (1936).
[31] H. Yukawa and S. Sakata, Inst. Phys. and Chem. Res. **686**, 187 (1937).

The ionization per cubic centimeter produced in an electroscope chamber per unit flux of radiation has been given as a function of the energy of the primary radiation up to 25 Mev by Streib, Fowler, and Lauritsen,[18] who extended the calculations of Laurence.[32] The calculation depends fundamentally on a theorem enunciated by Gray[33] that the energy equivalent of the ionization measured per cc in a cavity is equal to the energy converted per cc in the walls of the cavity divided by the relative stopping power for the secondaries of the wall material and of the gas filling the cavity. In considering scattering of the secondaries Laurence shows that extra traversals of the chamber compensate exactly from the scattering of the secondaries so that the calculations are much more simple than in the case of counters. Radiative loss corrections can also be made simply by omitting the energy radiated by the secondaries in the integral over the secondary energies.

a. Calculation of General Expressions for Counter Efficiency and Electroscope Ionization

The following derivation of counter efficiency and electroscope ionization will follow very closely the treatments by Bleuler and Zünti and by Laurence and will employ a common notation. In Fig. 12a is shown the detecting volume of a counter or electroscope surrounded by a wall of uniform material in which secondaries are produced by the incident radiation. The following assumptions are made:

1. The photoelectric effect is neglected; the Compton effect, pair formation, ionization loss, and radiative loss are considered.

2. The gamma-ray intensity is assumed to be uniform throughout the walls and cavity (plane beam). The absorption and scattering of the incident quanta in the walls is considered to be small. (A correction for this factor will ultimately be made.) Similarly, the building up of degraded, secondary radiation is at first neglected and a correction finally made.

3. The thickness of the walls exceed the ranges of the secondaries in the wall material.

4. The detecting volume is so small that the production of secondaries in it can be neglected and the change in energy of the secondaries in crossing it can be ignored.

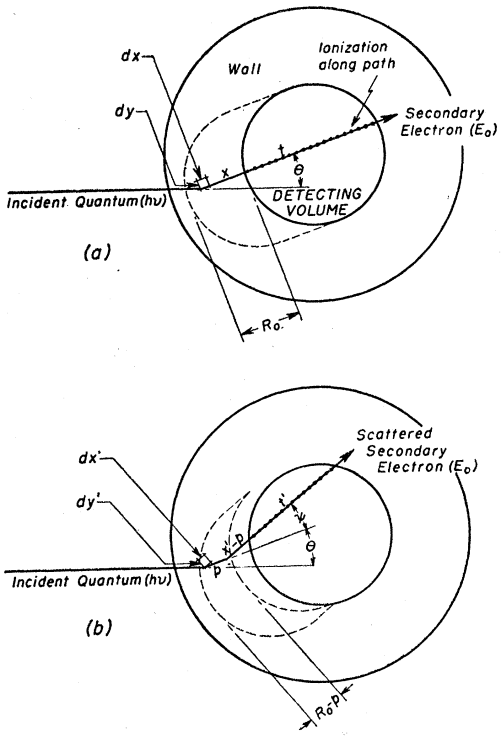

FIG. 12. The detection of secondaries produced by gamma-radiation.

Let the electronic cross section for transferring energy E_0 to a secondary electron in the wall in the direction given by the polar coordinates θ and ϕ by a quantum of energy $h\nu$ be $f_w(h\nu, E_0, \theta) \times \sin\theta d\theta d\phi dE_0$. Then the number of secondaries produced in a small element of the wall, $dxdydz$, by one quantum per sq. cm is

$$dN = n_w f_w \sin\theta d\theta d\phi dE_0 dx dy dz, \qquad (29)$$

where n_w is the number of electrons per cubic centimeter in the wall material. There may, of course, exist a functional relation between E_0 and θ, as in the Compton effect. On the other hand, E_0 may be related only on the average to θ, as in pair formation where the nucleus may take up an indeterminate recoil.

If the dN secondaries were to continue in a straight path without deflection, they would produce in the detecting volume a number of

[32] G. C. Laurence, Can. J. Research **A15**, 67 (1937).
[33] L. H. Gray, Proc. Roy. Soc. **A156**, 578 (1936).

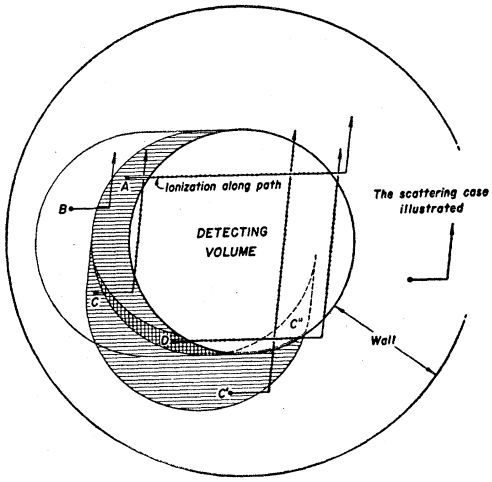

FIG. 13. Various parts of the wall of an electroscope or counter in which secondaries are produced by gamma-radiation.

ions, I, given in differential form by

$$dI=\frac{I}{w_g}(dE/dx)_g'tdN, \tag{30}$$

which on integration becomes

$$I=\frac{n_w}{w_g}\int\int\int f_w \sin\theta d\theta d\phi \times\int\int\int_0^{R_0}(dE/dx)_g'tdxdydzdE_0. \tag{31}$$

These same secondaries will produce a number of counts ϵ given in differential form by

$$d\epsilon=dN, \tag{32}$$

which upon integration becomes

$$\epsilon=n_w\int\int\int f_w \sin\theta d\theta d\phi\int\int\int_0^{R_0}dxdydzdE_0. \tag{33}$$

In these equations w_g is the energy required to produce an ion in the gas in the chamber (32.2 e-volts in air), $(dE/dx)_g'$ is the energy loss by collision in the gas, and t is the length of path across the detecting volume. The energy loss $(dE/dx)_g'$ is a function of the energy of the particle as it emerges into the chamber and is thus a function of the initial energy and the distance x measured along the path (here assumed straight) from the element of volume $dxdydz$ to the chamber. The integration over x will be from zero to R_0, the maximum range of the particles of energy E_0.

b. The Effect of the Scattering of Secondaries on Electroscope Ionization

In treating the effect of scattering on I, Laurence assumes that a fraction $gdpd\omega$ of the particles are elastically scattered after traveling a distance p as in Fig. 12b, in directions confined by the cone $d\omega$ making an angle ψ with the original direction. Then the inner triple integral of Eq. (31) must be increased by the addition of terms of the form

$$-gdpd\omega\int\int\int_p^{R_0}(dE/dx)_g'tdxdydz +gdpd\omega\int\int\int_p^{R_0}(dE/dx')_g't'dx'dy'dz',$$

in which x' is now the total distance traveled along the path of the secondary to the edge of the detecting volume, y' and z' are coordinates normal to the direction of the path after scattering, and t' is the distance across the chamber in the direction in which the particle emerges into the chamber. Laurence points out that both of the integrals in the above terms are equal to

$$V\int_p^{R_0}(dE/dx)_g'dx,$$

where

$$V=\int\int tdydz=\int\int t'dy'dz'$$

is the volume of the chamber. Hence the two additional terms cancel, and the total ionization is unaffected by nuclear scattering, and we have for the ionization per unit volume

$$i=\frac{I}{V}=\frac{n_w}{w}\int\int f_w \sin\theta d\theta d\phi \times\int\int_0^{R_0}(dE/dx)_g'dxdE_0. \tag{34}$$

The integral over x can be replaced by an integral over E, the energy of the secondary as it varies from E_0 to zero, by the substitution

$$dx=dE/(dE/dx)_w, \tag{35}$$

where $(dE/dx)_w$ is the loss of energy in the wall by both radiation and collision. It is convenient to substitute for the energy losses the electronic cross sections for energy loss, namely,

$$\lambda_g' = \frac{1}{n_g}(dE/dx)_g' \quad \text{and} \quad \lambda_w = \frac{1}{n_w}(dE/dx)_w.$$

We also note that the integral over x or E is independent of θ and ϕ, so that

$$i = \frac{n_g}{w_g}\int_0^{h\nu} \phi_w(h\nu, E_0)\int_0^{E_0}\left(\frac{\lambda_g'}{\lambda_w}\right)dE dE_0, \quad (36)$$

where

$$\phi_w(h\nu, E_0)dE_0 = dE_0\int\int f_w(h\nu, E_0, \theta)\sin\theta d\theta d\phi$$

is the differential electronic cross section for production of a secondary of energy E_0 by a quantum of energy $h\nu$. We take the integral over E_0 up to $h\nu$, even though ϕ_w vanishes for

$$E_0 > \frac{2h\nu}{2h\nu + mc^2}h\nu$$

for the Compton effect and for $E_0 > h\nu - 2mc^2$ for pair formation.

c. The Effect of the Scattering of Secondaries on Counter Efficiency

In applying Laurence's argument to the counter problem we can proceed as before to increase the triple integral of Eq. (33) by terms of the form

$$-gdpd\omega\int\int\int_p^{R_0} dxdydz + gdpd\omega\int\int\int_p^{R_0} dx'dy'dz'.$$

At first consideration it might seem that the two integrals in these terms reduce to $S(R_0-p)$ and $S'(R_0-p)$, where S and S' are the areas of the detecting volume projected on a plane normal to the direction in which the secondary enters the chamber. If this were the case, ϵ for a spherical counter would be independent of scattering, since the projected area of a sphere is the same in all directions. However, the integral in the second term is not equal to $S'(R_0-p)$, as can be seen from the illustration for an arbitrary single scattering shown in Fig. 13. In this figure $A+B$ would be the volume

$$\int\int\int_0^{R_0} dxdydz = SR_0$$

contributing secondaries to the counter if scattering were neglected. With the particular scattering we consider, particles from A can still reach the counter while those from B cannot (at least before being scattered). The loss of particles from B is partly compensated for by particles from C (or C') being scattered into the counter. The compensation would be exact if the region C'' fell in the wall and not in the detecting volume. In the case of the electroscope the compensation is exact even though no particles are produced in C'' because those from D (double cross hatched section of A) are scattered in the opposite wall and contribute additional ionization over their path after scattering. The counter, however, counts the particles from D only once, and thus the compensation is not complete and the counter reading is decreased by the scattering. In the counter case the integral over the region in the wall which supplies the scattered particles must be evaluated in such a way that re-entrant particles are counted only once.

It is clear that a relation of the type for i, Eq. (34), cannot be obtained for ϵ. That this is so is evident from the fact that Gray's theorem must only be applied to a detector whose response is proportional to the energy of the secondaries. It must not be applied to a detector which measures the number of secondaries. Instead we must take into account the decrease in number of electrons along a given direction because of scattering. The probability, P, that an electron of energy E_0 produced in $dxdydz$ at the angle θ, ϕ will pass through the counter is a function of all the variables E_0, x, y, z, θ and ϕ. We thus have

$$\epsilon = n_w\int\int\int\int\int\int f(h\nu, E_0, \theta) \times P(E_0, x, y, z, \theta, \phi)\sin\theta d\theta d\phi dxdydzdE_0. \quad (37)$$

Now for all y, z and θ, ϕ the dependence of P on E_0 and x will be largely the same. The variation

of P with x will exhibit the characteristic absorption of electrons out to the range $R_0(E_0)$, at which point P will vanish. Thus we can introduce with good physical argument, as well as formally, a value $\bar{P}(E_0, x)$ which has been averaged over the other variables with an appropriate weighting given by $f_w(h\nu, E_0, \theta)\sin\theta$. When we do this we note that the integral over $dydz$ must include all portions of the wall within a distance R_0 from the surface of the counter and not just the volume obtained by sweeping the projected area along a given direction. However, we must also note that for each direction of secondary emission described by θ and ϕ there are corresponding volume elements in the wall near the source of the radiation and in the opposite wall away from the source. Since $\bar{P}(E_0, x)$ has been averaged over the entire sphere around the point of secondary emission, only one of these volume elements must be considered. This will introduce a factor of $\frac{1}{2}$ in the calculations.

We are primarily interested in cylindrical counters with radiation incident upon them normal to the axis. Then it is convenient to replace x, y, and z by cylindrical coordinates ρ, ψ, z with origin on the axis of the counter. In this case if R_0 is small compared to the counter dimensions we obtain

$$\tfrac{1}{2}\int\int\int dxdydz = \tfrac{1}{2}\int\int\int \rho d\rho d\psi dz \approx 2\pi\rho_c l_c R_0, \quad (38)$$

where ρ_c and $2l_c$ are the radius and length of the counter, respectively. The quantity $4\rho_c l_c$ is just the projected area of the counter along the direction of incidence of the gamma-rays. Since ϵ is the number of counts per quantum per square cm we obtain for ϵ, the efficiency in counts per incident quantum the final expression:

$$\epsilon = \frac{\pi}{2} n_w \int_0^{h\nu} \phi_w(h\nu, E_0) \int_0^{R_0(E_0)} \bar{P}(E_0, x)dxdE_0. \quad (39)$$

This expression is identical with that given by Bradt *et al.*, who use the notation $2D(E_0, x)$ for $\bar{P}(E_0, x)$.

The quantity $\bar{P}(E_0, x)$ must be determined by a combination of experimental and theoretical investigations. However, under most circumstances it has been evaluated for a geometry quite dissimilar to that of Fig. 12. The usual arrangements are similar to those described in the previous section where the deviation of the path through the absorber from the normal is limited by the relative positions of source and detector to angles of the order of one radian or less. The relative values of

$$\int_0^{R_0} \bar{P}(E_0, x)dx$$

for the counter geometry and the usual experimental geometry depends essentially on the amount of scattering. We can make approximate calculations in two limiting cases. For very high energy quanta where the secondaries are projected mainly in the forward direction, where scattering can be neglected, and radiation and ionization give a true absorption along a straight line path, the result is independent of the geometrical arrangements. We must recall that the previous calculation of the integral over y and z will now give the projected area of the counter rather than $\pi/2$ times this area so that in this first limiting case

$$\epsilon = n_w \int_0^{h\nu} \phi_w(h\nu, E_0) \int_0^{R_0(E_0)} p(E_0, x)dxdE_0, \quad (40)$$

where $p(E_0, x)$ is the absorption function for electrons of energy E_0 as ordinarily determined experimentally. For low energy electrons where the scattering is very large the initial directions of ejection are unimportant, and the production of secondaries can be considered to be isotropic. In fact, we can consider the secondaries to radiate in straight lines in all directions from the point of emission. It is also satisfactory to assume that all the secondaries have just the average range, $\bar{R}(E_0)$. In this second case, in considering electrons emitted at a depth x in the counter wall we must consider the average penetration for all particles starting toward the counter within a cone of half-angle given by $\arccos(x/\bar{R})$. In the ordinary experimental arrangement we must, on the other hand, average over the cone of this same half-angle or of the half-angle established by the geometry of detection, whichever is the smaller. In the counter problem the half-angle of detection is of course just $\pi/2$. Thus in the

counter case the penetration is to be averaged over longer paths in general, and will be smaller than that ordinarily measured. As indicated by Bleuler and Zünti, rough calculations of these average penetrations and then substitutions in the integrals over the penetrations indicate that the ratio of

$$\int \bar{P}(E_0, x)dx \quad \text{to} \quad \int p(E_0, x)dx$$

is between $\frac{1}{2}$ and unity. This factor will approximately cancel the $\pi/2$ in expression (39) and Eq. (40) will hold approximately. Furthermore, Bleuler and Zünti have shown that Eq. (40) gives results in agreement with experiment in the low energy region. There is no reason to believe that the integrals will differ markedly at intermediate energies and hence we will employ it in our calculations over the entire energy range from 2 to 25 Mev.

d. Simplified Integral Expressions for i and ϵ

The expressions for i and ϵ can be written

$$i=\frac{n_g}{w_g}\int_0^{h\nu}\phi_w(h\nu, E_0)E_0\left\langle\frac{\lambda_g'}{\lambda_w}\right\rangle_{Av}dE_0, \tag{41}$$

$$\epsilon=n_w\int_0^{h\nu}\phi(h\nu, E_0)\bar{R}(E_0)dE_0, \tag{42}$$

where

$$\bar{R}(E_0)=\int_0^{R_0(E_0)}p(E_0, x)dx$$

and

$$\left\langle\frac{\lambda_g'}{\lambda_w}\right\rangle_{Av}=\frac{1}{E_0}\int_0^{E_0}\left(\frac{\lambda_g'}{\lambda_w}\right)dE.$$

In these equations the ratio of the stopping cross sections must be averaged over the energy of the secondary particle and the penetration function over its range. In Eq. (42) $\bar{R}(E_0)$ is just the average range for a secondary of energy E_0 along the original direction of motion as determined by the usual experimental arrangement. Since $\lambda_g'/\lambda_w\approx 1$ Eqs. (41) and (42) reduce to the expressions

$$i=\frac{n_g}{w_g}\sigma_w\bar{E}(h\nu) \tag{43}$$

and

$$\epsilon=n_w\sigma_w\bar{r}(h\nu), \tag{44}$$

where

$$\sigma_w=\int_0^{h\nu}\phi_w(h\nu, E_0)dE_0$$

is the total electronic cross section for the production of secondaries in the wall, $\bar{E}(h\nu)$ is the average energy of the secondaries produced by a quantum of energy $h\nu$, and $\bar{r}(h\nu)$ is the average over their energy distribution of the average range of these secondaries. These expressions have been employed by many investigators in estimates of gamma-ray intensity from electroscope and counter measurements. We attempt here to calculate the appropriate averages somewhat more accurately than has been done in the past for high energy gamma-rays.

e. Electroscope Ionization

We will first discuss the electroscope ionization. Using Bloch's formula for the stopping from ionization by collision and approximating to the stopping by radiation for the domain 2–25 Mev, by

$$\lambda''/\lambda=(\lambda-\lambda')/\lambda\approx EZ/2000mc^2, \tag{45}$$

where E is the electron energy and the double primes indicate radiation effects, we get

$$\frac{\lambda_g'}{\lambda_w}\approx 1-\frac{EZ_w}{2000mc^2}+\frac{2}{3}\frac{\ln(Z_w/Z_g)}{\ln(E/A)}, \tag{46}$$

where $A=(2mc^2I_0^2)^{\frac{1}{2}}=580$ e-volts with $I_0=13.6$ ev, the ionization potential of hydrogen. This expression must be averaged, for each secondary, over its energy and then over the initial energy distribution of the secondaries produced in the solid medium. The first average is

$$\left\langle\frac{\lambda_g'}{\lambda_w}\right\rangle_{Av}\approx 1-\frac{EZ_w}{4000mc^2}+\frac{2}{23}\ln\frac{Z_w}{Z_g}, \tag{47}$$

where the factor 2/23 is a good average value in the domain under discussion.

We now need to know $\phi_w(h\nu, E_0)dE_0$, the cross section for producing a secondary of energy E_0 in the medium. If we set $f=E_0/h\nu$ and $k=h\nu/mc^2$, the Klein-Nishina formula and the cross section for pair formation give at high energies:

$$\phi_w(k, f)df=\pi r_0^2df\left[\frac{1}{k}\left(1-f+\frac{1}{1-f}\right)+1.65\frac{Z_w}{137}\frac{k}{k-2}\ln\frac{k}{4.3}\right], \tag{48}$$

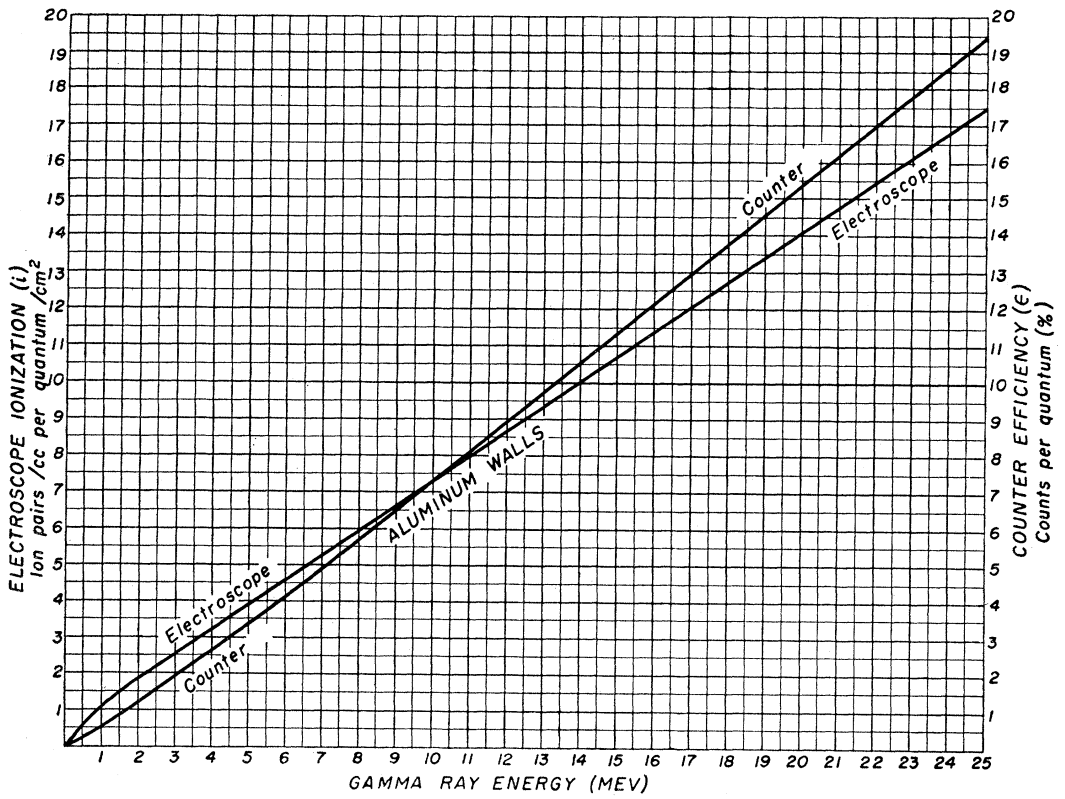

FIG. 14. Counter efficiency and electroscope ionization as a function of gamma-ray energy.

where $r_0=e^2/mc^2$ and where the second term which is for pair production is an empirical fit to Heitler's[17] curve for pair production in the region from 2 to 25 Mev.

The remaining procedure is to integrate $E_0\langle\lambda_g'/\lambda_w\rangle_{Av}$ over the differential cross section. The results are plotted in Fig. 14 for aluminum walls and an air cavity ($Z_g=7.2$) and are given in good numerical approximation for $Z_w<20$ and $h\nu<25$ Mev by

$$i=\frac{n_g}{w_g}\left(1+\frac{2}{23}\ln\frac{Z_w}{Z_g}-\frac{h\nu Z_w}{5000mc^2}\right)\sigma_w\bar{E}, \quad (49)$$

which is more exact than Eq. (43). It is convenient to combine terms in a somewhat different manner and to write:

$$i=\frac{n_g}{w_g}\left(1+\frac{2}{23}\ln\frac{Z_w}{Z_g}\right){}_a\sigma_w'h\nu. \quad (50)$$

In this alternative expression ${}_a\sigma_w'$ is the true energy absorption coefficient per electron for the wall material and is given by

$${}_a\sigma_w'=\left(1-\frac{h\nu Z_w}{5000mc^2}\right){}_a\sigma_w$$

$$=\pi r_0{}^2\frac{mc^2}{h\nu}\left(1-\frac{h\nu Z_w}{5000mc^2}\right)\left(\ln\frac{h\nu}{1.1mc^2}+\frac{(h\nu-2mc^2)Z_w}{165mc^2}\ln\frac{h\nu}{4.3mc^2}\right). \quad (51)$$

Equation (49) contains $\bar{E}$, the average energy of the secondary electrons. It is given analytically by $\bar{E}=({}_a\sigma_w/\sigma_w)h\nu$ with ${}_a\sigma_w$ given by Eq. (51) and σ_w given by summing the two cross sections evaluated in Eqs. (22) and (23). For aluminum walls we find

$$\bar{E}=0.55h\nu \quad (52)$$

within a few percent over the entire energy range from 2.5 to 25 Mev.

For $Z_w=20$ and $h\nu=25$ Mev the expression for ${}_a\sigma_w'$ is correct to about 5 percent. To extend

this treatment to higher Z_w and $h\nu$ would require giving up Gray's theorem, since then it is no longer possible to treat the range of the electrons as small, that of the gamma-rays as large, compared to the dimensions of the surrounding medium.

In order to make yield determinations from the reading of an electroscope its charge sensitivity in divisions per ion pair per cc must be known. The voltage sensitivity can, of course, be determined very simply. Direct measurement of the charge sensitivity involves a determination of the capacity of the electroscope which for the type used in these experiments is less than one cm. There is an additional difficulty in that the recombination reduces the efficiency of ion collection to less than 100 percent. For these reasons it is preferable to measure the charge sensitivity by determining the electroscope response to radiation of known intensity. We have employed two radium standards, certified by the National Research Council of Canada, to contain 0.21 and 1.74 milligrams of radium. Laurence has given an empirical expression for the strength of a unit radium source filtered by platinum of thickness t greater than 0.3 mm as follows:

$$s=5.91(1-0.13t)\times 10^6 \text{ ion pairs per cc/mg sec. per cm}^2$$

for t in millimeters. Using this value, we have found the reciprocal sensitivity of the two electroscopes used in the experiments described below to be 1.26×10^4 ion pairs per cc per division and 1.20×10^4 ion pairs per cc per division. The ordinates of Fig. 14 can be converted into divisions per incident quantum per cm^2 by dividing by these factors.

f. Counter Efficiency

1. Range of Electrons

Turning to the counter calculations it is clear that R_0, the range of high energy electrons, must first be established. This will be the maximum range of homogeneous electrons and is essentially the total distance along the path traversed by an electron (which does not radiate) in being stopped in the wall. It is given by

$$R_0=\int_0^{E_0}\frac{dx}{(dE/dx)_w'}, \tag{53}$$

where $(dE/dx)_w'$ is the energy loss by ionization in the walls. It is true that radiation involves energy loss, but this does not affect the maximum range since radiative processes are relatively improbable for the energies under consideration and, in general, radiation results in large energy losses by a relatively few particles rather than small losses by the majority.

Many experimental and theoretical determinations of R_0 in the range below 3 Mev have been made and are summarized by Bleuler and Zünti.[22] The semi-empirical curve for aluminum which they finally adopt in their calculations is given within 0.01 cm by the expression

$$R_0=0.24E_0\frac{E_0+mc^2}{E_0+2mc^2}\text{ cm} \tag{54}$$

for E_0 and mc^2 in Mev. The derivative of this expression with energy fits the theoretical energy loss curve only moderately well at very low energies but is a good approximation above 1 Mev. In extending the range curve to higher energies we will integrate over the theoretical energy loss but adjust the constant of integration by using Bleuler and Zünti's value at 3 Mev.

In the high energy region Heitler[17] gives the energy loss by ionization of an electron of total energy $W=E+mc^2$ as

$$\left(\frac{dE}{dx}\right)_w'=\xi\ln\beta W, \tag{55}$$

where

$$\xi=6\pi r_0^2 n_w mc^2=0.60 \text{ Mev/cm for aluminum,}$$

and

$$\beta=(2mc^2I_0^2Z_w^2)^{-\frac{1}{2}}=316 \text{ Mev}^{-1} \text{ for aluminum.}$$

Hence in terms of a standard range, R_s, at energy, W_s,

$$\begin{aligned}R_0-R_s&=\int_{W_s}^{W_0}\frac{dW}{\xi\ln\beta W}\\&=\frac{1}{\xi\beta}[\bar{E}i(\ln\beta W_0)-\bar{E}i(\ln\beta W_s)]\\&=\frac{1}{190}[\bar{E}i(\ln316W_0)-\bar{E}i(\ln316W_s)]\end{aligned} \tag{56}$$

for aluminum with range in cm and energy in

Mev. In these expressions $\bar{E}i$ represents the exponential integral.

If we take from Bleuler and Zünti $R_s=0.62$ cm for $E_s=2.96$ Mev, $W_s=3.47$ Mev, we obtain

$$R_0=\frac{1}{190}\bar{E}i(\ln 316W_0)-0.39 \text{ cm}. \tag{57}$$

This relation as well as Bleuler and Zünti's curve up to 3 Mev is plotted in Fig. 15. It is given approximately by

$$R_0=E_0/4.8 \text{ cm} \tag{57'}$$

for R_0 in cm and E_0 in Mev. For the so-called "practical" maximum or "extrapolated" range of homogeneous electrons which in the low energy region is given by

$$R_p=0.22E_0\frac{E_0+mc^2}{E_0+2mc^2} \text{ cm}, \tag{58}$$

we find by the same methods

$$R_p=\frac{1}{190}\bar{E}i(\ln 316W_0)-0.44 \text{ cm}. \tag{59}$$

2. *The Penetration of Electrons*

Few of the electrons of energy E_0 attain the maximum range R_0, primarily because of scattering and in part because of radiation. An initially parallel beam of electrons of homogeneous energy is widened by multiple scattering, and the number moving in directions within any cone about the original direction becomes smaller with distance. Eventually the divergence of the beam becomes so large that the problem becomes similar to a diffusion problem and an "apparent" absorption coefficient can be employed profitably in the calculations. Superimposed throughout is the gradual loss of particles because of radiation. Before diffusion sets in the probability of an electron of energy E remaining within a cone of angle ϕ after traveling a distance x is given from multiple scattering theory by:

$$p(E, x)=1-\int_{\phi}^{\infty}\frac{\theta}{\lambda^2}e^{-\theta^2/2\lambda^2}d\theta=1-e^{-\phi^2/2\lambda^2}, \tag{60}$$

where, according to Bothe,[34] the most probable scattering angle is given by

$$\lambda(E, x)=(4\pi r_0^2N_wZ_w^2)^{\frac{1}{2}}\left(\frac{2mc^2}{E}\cdot\frac{E+mc^2}{E+2mc^2}\right)x^{\frac{1}{2}} \approx c\frac{x^{\frac{1}{2}}}{W}, \tag{61}$$

where N_w is the number of atoms per cc in the wall and where the constant, c, has the value 3.29 in aluminum. We wish to determine the absorption curve for electrons of initial total energy, $W_0=E_0+mc^2$, which lose energy as they traverse the absorber x. The square of the most probable scattering angle is proportional to the mean square scattering. The mean square scattering in x is equal to the sum of the mean square scatterings in each element dx, and so we have

$$\lambda^2(E_0, x)=\int_0^x\frac{c^2dx}{W^2}. \tag{62}$$

For high energy particles we can set the energy loss equal to a constant $k\approx 4.8$ Mev/cm in aluminum so that $W=W_0-kx$ and

$$\lambda^2(E_0, x)=\frac{c^2x}{W_0(W_0-kx)}. \tag{63}$$

This is to be substituted in (60) to give $p(E_0, x)$. For commonly used experimental arrangements $\phi\sim 1$ radian, so we have, finally,

$$\begin{aligned}p(E_0, x)&=1-\exp[-(W_0(W_0-kx)/2c^2x)]\\&=1-\exp[-(W_0(W_0-4.8x)/21.6x)]\end{aligned} \quad \text{in aluminum.} \tag{64}$$

The above expression will hold until λ becomes so large that diffusion sets in. This occurs at the limiting value $\lambda_d=0.576$ radian[22] so that the amount of penetration, x_d, over which Eq. (64) holds is given by

$$x_d=\frac{\lambda_d^2W_0^2}{c^2+\lambda_d^2W_0k}. \tag{65}$$

For aluminum this reduces to

$$x_d=\frac{E_0+1}{E_0+7.5}R_0, \tag{66}$$

[34] W. Bothe, *Handbuch der Physik* **22/2**, 1 (1933).

if we substitute $k=E_0/R_0$ and $W_0=E_0+0.5$. Figure 15 shows x_d in comparison with R_0.

In the diffusion region Bothe[34] has introduced an apparent absorption coefficient equal to $1.3\lambda^2/x$ so that

$$\frac{1}{p}\frac{dp}{dx}=-1.3\frac{\lambda^2}{x}\approx 1.3\frac{c^2}{E^2}\approx 1.3\frac{c^2}{k^2R^2} \approx\frac{0.6}{R^2}\text{ in aluminum,} \tag{67}$$

where $E=E(E_0, x)$ is the energy remaining after penetration through the distance x. On integration

$$p(E_0, x)=p_d\exp\left[-1.3\frac{c^2}{K^2}\left(\frac{1}{R}-\frac{1}{R_d}\right)\right] =p_d\exp\left[-0.6\left(\frac{1}{R}-\frac{1}{R_d}\right)\right]\text{ in aluminum,} \tag{68}$$

where R is the residual range R_0-x, $R_d=R_0-x_d$, and $p_d=p(E_0, x_d)$. Equation (68) must be smoothly fitted to Eq. (64) in the region near x_d where diffusion sets in

Throughout the range the effect of radiation must be superimposed on the scattering given by the above expressions. The atomic cross section for radiation is defined by Heitler[17] in the

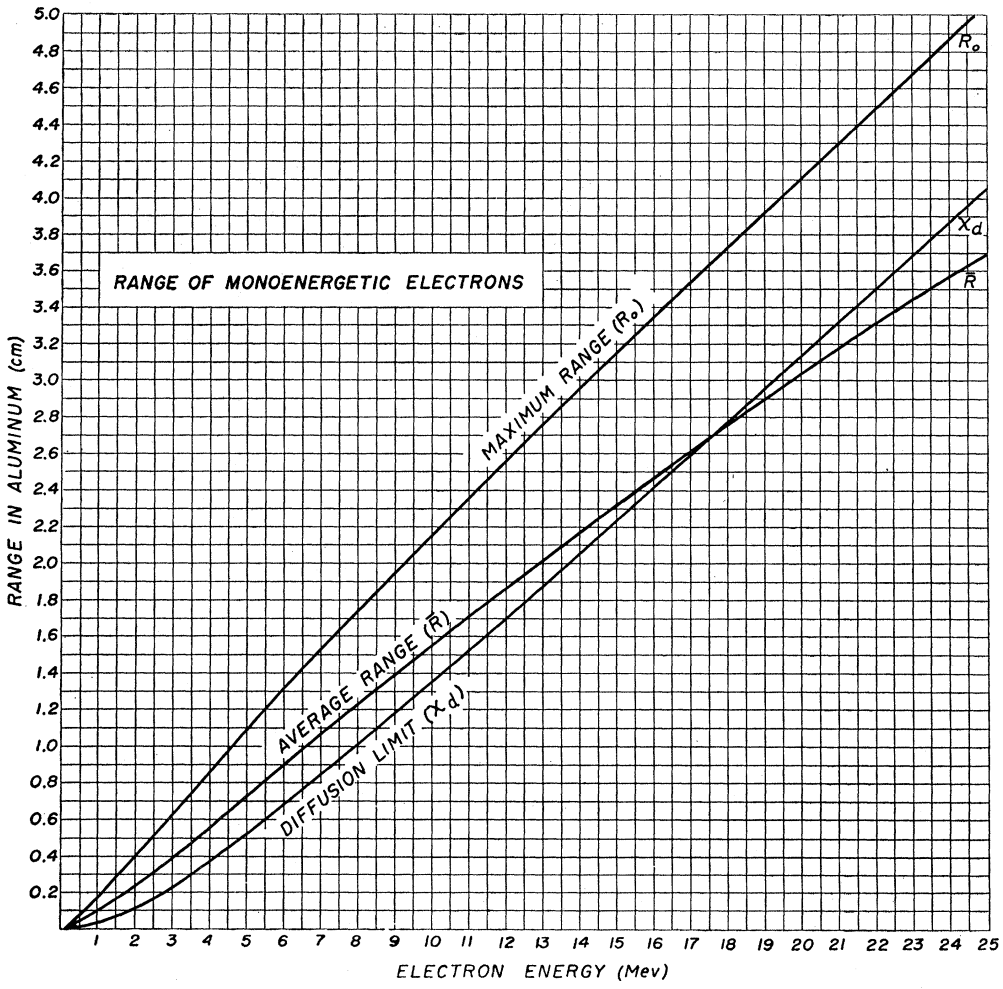

FIG. 15. The maximum and average ranges in aluminum of monoenergetic electrons. Also illustrated is the range at which complete diffusion sets in.

equation

$$\frac{1}{E}\left(\frac{dE}{dx}\right)''_{w}=N_w\phi_{\rm rad}. \tag{69}$$

It is given approximately in the energy range under consideration by the constant value

$$\phi_{\rm rad}\approx 3\pi r_0^2 Z_w^2, \tag{70}$$

where r_0 is the classical electron radius.

Since radiation usually results in a loss of a large proportion of the electron's energy, we can write

$$\frac{1}{p}\frac{dp}{dx}=-f(x)-h, \tag{71}$$

where $f(x)$ represents any arbitrary effect of scattering and

$$h=N_w\phi_{\rm rad}=0.065\ \text{cm}^{-1}\ \text{for aluminum}. \tag{72}$$

The integration of (71) can be carried out in a simple manner for any given function $f(x)$, and we obtain

$$p=e^{-hx}e^{-\int f(x)dx}. \tag{73}$$

Equations (64) and (68) must then be multiplied by

$$e^{-hx}=e^{-h(R_0-R)}\approx 1-h(R_0-R)$$

in order to include radiation effects.

The results of calculations employing these equations are given for 17.5-Mev, 6.3-Mev, and 2.6-Mev radiation in Fig. 16. We note from the form of Eq. (68) that the diffuse scattering yields a "universal" curve for all initial ranges, if we normalize to unity at very large R. Starting at any range R_d, the relative behavior of $p(E_0, x)$ as a function of x is given by following the curve to the right. To obtain the absolute probability one must, of course, normalize the original point to unity. The effect of radiation on the diffuse scattering curve can also be depicted in a "universal" fashion by multiplying by e^{+hR} rather than e^{-hx}. This has been done in the upper curve of Fig. 16. To obtain the curve for a particular energy we must adjust Eq. (64) to the radiation diffusion curve. This has been illustrated in the figure for three energies. For low energies the approximations for λ^2/x in Eq. (67) are not valid, and we have shown the results of Bleuler and Zünti in the region below 0.6 cm.

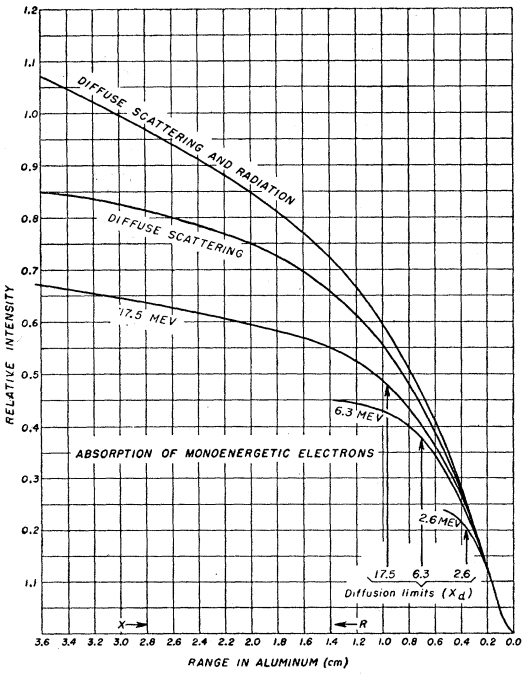

FIG. 16. The absorption of monoenergetic electrons.

3. *The Counter Efficiency Integral*

In order to determine ϵ, the integral of $p(E_0, x)$ over the range must be evaluated from the curves of Fig. 16, that is, we must determine $\bar{R}(E_0)$. It is clear from the shape of the curves that to first-order terms this will be given by

$$\bar{R}(E_0)=\int_0^{R_0} p(E_0,x)dx=C_1x_d+\tfrac{1}{2}C_2(R_0-x_d), \tag{74}$$

where C_1 and C_2 are constants which are somewhat less than unity. Neglecting radiation we have found $C_1=C_2=0.94$, the numerical value being determined from graphical integration of the 17.5- and 6.3-Mev curves. Hence

$$\bar{R}(E_0)=0.47(R_0+x_d)$$
(neglecting radiation). (75)

Expression (75) will be in error at low energies since $C_2<0.94$ in this region, and it is preferable to employ the calculations of Bleuler and Zünti at low energies. The radiation correction will, of course, depend on the exact shape of the absorption curve and more specifically on the

ratio of x_d to R_0, but to a first-order approximation it will introduce a term $1-h\bar{R}/2$ so that

$$\bar{R}(E_0)=0.47(R_0+x_d)-0.007(R_0+x_d)^2 \quad \text{(including radiation)}. \quad (76)$$

This average range is illustrated in Fig. 15.

4. Average Over the Secondary Energy Distribution

The final determination of ϵ involves the averaging of $\bar{R}(E_0)$ over the energy distribution $\phi(h\nu, E_0)$ of the secondaries. This again must be done graphically or by very approximate analytical methods. Since $\bar{E}$ has been computed in the determination of i, we have made the approximation $\bar{r}(h\nu)=\bar{R}(\bar{E})$ and have determined the latter quantity for substitution in the expression for ϵ. The values for $\bar{r}(h\nu)$ are given in Fig. 10, and ϵ is plotted with i in Fig. 14. It will be noted that the ratio of ϵ to i increases with increasing energy as the scattering, which decreases only ϵ, becomes smaller and smaller. In the limiting case of no scattering we have the relation

$$\lim(\epsilon/i)=1.37 \text{ (aluminum walls)} \quad (77)$$

for ϵ in percent and i in ions/cc per quantum/cm^2. In the energy region of interest this ratio varies from 0.69 at 2.6 Mev to 1.10 at 17.5 Mev.

5. Application to Coincidence Counter Measurements

The expressions which we have derived for $p(E_0, x)$ can be substituted into Eq. (27) to give the absorption curves to be expected in coincidence counter arrangements. We have not carried out detailed calculations of this type, but it is clear the calculated curves will be of the form observed experimentally as shown in Figs. 7–11. Allowing some latitude in the choice of ϕ, the half-angle of the cone of detection, it is anticipated that a good fit to the experimental results can be obtained. Bleuler and Zünti have done this at low energies satisfactorily. In our coincidence counter arrangement ϕ is somewhat larger than in theirs. However, in the counter efficiency calculations we have employed curves for $p(E_0, x)$ similar to theirs, since they have shown experimentally at low energies that the factor $\pi/2$ in Eq. (39) is then cancelled almost exactly on going from $\bar{P}(E_0, x)$ to $p(E_0, x)$.

f. Absorption of the Primary Radiation: Building up of Secondary Radiation

The derivations given above permit calculation of ϵ or i only when the energy and composition of the radiation in the wall is strictly known. In actual practice we wish to know the ionization produced by a monochromatic gamma-ray falling on the external walls, and some question may arise as to the complications arising from the building up of secondary radiation from the Compton effect, radiation of the secondary electrons, and annihilation of positron members of pairs. The answer to this question depends on the geometry of the experiment and only in case the secondary quanta produced in the walls and escaping therefrom are completely compensated for by scattering in surrounding material can a definite answer be given. Fortunately, almost complete compensation is attained by surrounding the electroscope or counter on all sides by walls thicker than the range of the secondary electrons in the wall material. A further simplification arises from the fact that $\bar{E}/h\nu$ and $\bar{r}(h\nu)/h\nu$ are roughly independent of energy. For the electroscopes the argument can be continued as follows. If $\psi(E)dE$ is the distribution in energy of quanta in the walls near the sensitive volume produced by monochromatic quanta falling on the external walls, then the energy conversion per unit volume is

$$n_w\int {}_a\sigma_w'(E)\psi(E)EdE.$$

For ${}_a\sigma_w'=$ constant this becomes ${}_a\sigma_w'n_wW$, where W is the energy remaining in the form of radiation after the quanta have penetrated to a point where their secondaries can reach the electroscope. Since secondaries are produced at all points in the wall surrounding the cavity we can write $W=W_0\exp(-{}_a\sigma_w'n_wt)$, where t is the wall thickness. Actually ${}_a\sigma_w'$ is not strictly constant, but we may use the expression by inserting the appropriate value of ${}_a\sigma_w'$ for the incident radiation in question. For counters a similar approximate correction can be made.

g. Geometrical Corrections in Solid Angle Calculations

Yield measurements are usually made with the highest possible intensity at the detector.

TABLE III. Solid angle correction factors.

Source	$h\nu$ (Mev)	Electroscope readings $\rho=2.8$ cm; $l=3.4$ cm; $R=7.9$ cm	Counter readings $\rho=0.9$ cm; $l=3.8$ cm; $R=7.9$ cm
ThC″	2.6	0.98	1.07
$F(p\alpha', \gamma)$	6.3	0.96	1.05
$Li(p\gamma)$	17.5	0.94	1.03

This often means that the electroscope or counter are used at distances from the source which are comparable to their dimensions. The assumption of uniform intensity in the walls is thus not true even if absorption is neglected. The correction to be made to observations because of this effect cannot be calculated unless the relative effectiveness of each element of the wall in producing secondaries is known. For low energy radiation when scattering is large, the relative effectiveness is about the same for all elements of the wall, front, back, and sides. For high energy radiation it would be expected that the front walls, i.e., those nearest the source, would be the most effective. It is, of course, possible to compute the corrections by assuming various analytical functions for the dependence of the effectiveness on the position in the wall and carrying out the necessary integrations employing the inverse square law for the dependence on the distance from the source. In the case of a spherical detecting volume the function $\cos^n\theta/2$ is convenient where θ is the co-latitude of the element of wall measured with respect to an axis drawn from the center of the sphere to the source. If $\alpha=r/R$ is the ratio of the radius of the sphere to the distance from its center to the source, then we find that the ratio of the reading at R to that at large distances after both are corrected for the inverse law is

$$\frac{I(R)}{I(\infty)}=1+\frac{1}{3}\alpha^2+\frac{1}{5}\alpha^4+\cdots \quad (n=0) \qquad (78)$$

$$=1+\frac{2}{5}\alpha+\frac{9}{35}\alpha^2+\cdots \quad (n=1) \qquad (78')$$

$$=1+\frac{2}{3}\alpha+\frac{1}{3}\alpha^2+\cdots \quad (n=2). \qquad (78'')$$

The introduction of terms linear in $\alpha=r/R$ is apparent for the cases where the front walls are favored ($n>0$). The case of a cylinder can be easily computed when all elements of the wall are considered equally effective ($n=0$). If ρ is the radius of the cylinder and $2l$ is its length, then for the source at a distance R on a line normal to the cylinder axis at the center we find

$$\frac{I(R)}{I(\infty)}=1-\frac{1}{3}\frac{l^2}{R^2}\left(1+\frac{3}{2}\frac{\rho}{l}\right)\left(1+\frac{1}{2}\frac{\rho}{l}\right)^{-1}+\frac{\rho^2}{R^2}\left(1+\frac{1}{4}\frac{\rho}{l}\right)\left(1+\frac{1}{2}\frac{\rho}{l}\right)^{-1}+\cdots \qquad (79)$$

$$=1+0.06\frac{l^2}{R^2}+\cdots$$

for $R>l=1.2\rho$ (electroscope) (79′)

$$=1-0.35\frac{l^2}{R^2}+\cdots$$

for $R>l=4.2\rho$ (counter). (79″)

The introduction of positive linear terms in ρ/R and l/R is to be expected if the relative effectiveness for front walls is made greater than that for side and rear walls.

TABLE IV. Relative sensitivity of lead and aluminum lined detectors.

Source	Energy Mev	Pb wall/Al wall sensitivity electroscope	counter
$C^{12}(p\gamma)$	2.3	—	1.29
ThC″	2.6	1.28	1.26
$C^{13}(p\gamma)$	2.3, 5.8, 8.1	—	1.55
$F^{19}(p\alpha', \gamma)$	6.3	1.58	1.53
$Be^9(p\gamma)$	7.4	1.53	1.55
$Li^7(p\gamma)$	17.5	1.82	1.80

We have made an experimental investigation of these geometrical factors for 2.6-, 6.3-, and 17.5-Mev radiation, using an aluminum-lined cylindrical electroscope for which $l=1.2\rho$ and an aluminum-lined cylindrical counter for which $l=4.2\rho$. It was only possible to obtain reliable readings over a variation in intensity by a factor of 10 so that the results were not conclusive. The results could be fitted by expressions (79′) and (79″), with the addition of small positive linear terms being indicated for the higher energy radiation. The order of magnitude of the corrections is indicated in Table III, where the

empirical correction factors actually employed in the yield calculations of Section 7a are given. The correction factors are equal to $I(\infty)/I(R)$.

h. Angular Distribution of the Gamma-Radiation

The angular distribution of the gamma-radiation from $Li^7(p\gamma)$ has been found to be isotropic by Ageno[35] *et al.*, using protons with an energy of 500 kev. The distribution of the radiation from $F^{19}(p\alpha', \gamma)$ has been found to be isotropic by Van Allen and Smith,[36] using thick targets at bombarding energies of 370, 900, and 1000 kev. We have measured the relative intensity of the radiation from $Be^9(p\gamma)$ at 0°, 45°, and 90° at both the 988- and 1077-kev resonances. We find the results at the three angles to be the same within ±20 percent. As will be discussed below, there are good reasons to believe that the resonances in the $C^{12}(p\gamma)$ and $C^{13}(p\gamma)$ reactions are due to *s*-capture and thus that the radiation should be isotropic. In all the yield determinations which are described below, the intensity has actually been measured at 90° with the incident beam with the detectors subtending angles of ±25° in the plane of the beam, and the calculations have then been made by assuming the radiation to be isotropic. Since the intensity cannot vary in azimuth we have actually determined the yield over a considerable portion of the sphere (~40 percent). The yield results will not be changed markedly even if some deviation from isotropy is discovered in the reactions under consideration.

7. RESULTS OF YIELD MEASUREMENTS

a. Thick Target Yields

The yield of a nuclear reaction can be determined from measurements with thin or thick targets. For thin targets accurate measurements must be made of the mass per unit area. For thick targets the stopping power of the target materials must be known. Absorption in targets thick enough to stop the incident particles is negligible for gamma-radiation. Deterioration of targets and the effect of contaminations are relatively more serious for thin targets. We have found thick target results to be somewhat more reliable than those from thin targets, and the yields presented here are from thick target measurements. The targets employed were LiOH with the natural Li^6/Li^7 abundance, Be metal, Acheson graphite with the natural C^{12}/C^{13} abundance, and CaF_2. Deterioration of the targets was observed in the case of LiOH and CaF_2 under prolonged bombardment, and the results given are those found for freshly prepared targets with the minimum amount of bombardment necessary to establish the yield.

The thick target yields have been determined simultaneously with electroscopes and counters. Both lead and aluminum walls were employed. The results obtained with the electroscopes and counter having aluminum walls were employed to give the absolute yields. The experimental ratios of lead wall detection to aluminum wall detection have also been determined and are listed in Table IV. The theoretical calculations for lead-lined detectors are difficult to make, and the experimental ratios can be considered as a calibration for lead-lined detectors. Lead is often convenient in studying high energy radiation where the secondary ranges are relatively large because the thickness corresponding to the full range of the secondaries is considerably smaller in lead than in lighter materials such as aluminum.

The total charge incident on the target during the yield measurements was determined by collecting the charge in a condenser of small leakage and known capacity and measuring the voltage developed on the condenser by a calibrated quartz-fiber electrometer.

The results are included in Table I. The yields are in disintegrations per incident proton for the actual targets employed (LiOH, Be, C, CaF_2). In the case of $C^{13}(p\gamma)$ there are 50 percent more quanta than disintegrations, since the disintegration branches about equally to give one 8.1-Mev quantum and one 2.3-Mev quantum followed by a 5.8-Mev quantum.[3] Although we have employed the efficiencies corresponding to these energies, it is well to note that the approximate linearity of the detector sensitivity curves with energy makes the yield in disintegrations per incident particle relatively independent of

[35] M. Ageno, E. Amaldi, D. Bocciarelli, and G. C. Trabacchi, Ricerca Scient. 12, 139 (1941).
[36] J. A. Van Allen and N. M. Smith, Jr., Phys. Rev. 59, 501 (1941).

TABLE V. Radiation widths, proton widths, and proton widths at 1 Mev without barrier.

Source	E_R kev	$\omega\Gamma_\gamma$ ev	Γ_p kev	Γ_0 (kev) s-wave	p-wave	d-wave
$Li^7(p\gamma)$	439	8.9	12	70	540	1920
$Be^9(p\gamma)$	988	~12.5	~94	~230	~800	~11300
	1077	0.77	4	10	30	380
$C^{12}(p\gamma)$	453	0.63	35	1680	10500	—
$C^{13}(p\gamma)$	550	15	40	880	5000	—

the branching or the number of steps in the radiation as long as the total energy radiated in the various types of transitions is the same. In the case of $C^{12}(p\gamma)$ radioactive N^{13} is produced, and the effects of the two annihilation quanta must be taken into account in determining counter or electroscope sensitivities.

The agreement between electroscope and counter yields is satisfactory, and in further calculations their average has been employed. In the case of $C^{12}(p\gamma)$ the positron yield has also been measured with counters and is in agreement with the quantum yield. In the $F(p\alpha', \gamma)$ reaction the yield values are 20 percent higher than that given for the alpha-particles by Van Allen and Smith[36] ($1.43\times10^{-8}\alpha'/p$), and further studies of this discrepancy are contemplated. Our results are generally in good agreement with previous yield and width measurements.[2, 9, 18, 37]

TABLE VI. Alpha-particle widths, proton widths, and proton widths at 1 Mev without barrier.

E_R kev	Γ_α kev	$\omega\Gamma_p$ ev	$\omega\Gamma_0$ (kev) s-wave	p-wave	d-wave
		$F^{19}(p\alpha', \gamma)$			
338	4	30	150	660	1500
479	~5	10	4.5	16	330
589	~15	49	7.9	27	490
660	~5	96	7.7	27	430
820	7.6	32	1.0	3.2	45
862	5.2	830	19	66	750
890	4.8	27	0.5	1.6	20
927	8.0	475	8.1	25	285
1076	<1.2	7	0.06	0.1	1.3
1107	30	170	1.4	4.2	42
1122	4.1	27	0.2	0.6	6.0
1161	50	298	2.2	6.0	60
1274	19	343	1.7	4.8	45
1335	4.8	370	1.8	4.6	44
1363	15	3140	14	35	310
		$F^{19}(p\alpha'', \pi)$			
832	28	12	0.4	1.2	15
1100	70	28	0.2	0.7	70
1220	85	132	0.8	2.6	26
1362	36	210	1.0	2.3	21
		$F^{19}(p\alpha)$			
720	—	4	0.2	0.6	8
840	28	4	0.1	0.4	4.4
~1050	>100	50	0.5	1.5	15
1350	36	100	0.5	1.2	11

b. Discussion

From the absolute thick target yields it is possible to compute the term $\omega\gamma=\omega\Gamma_p\Gamma_x/\Gamma=2\epsilon Y/\lambda^2$ which appears in the Breit-Wigner formula. The quantity ω is the statistical factor, Γ_p is the width for re-emission of a proton, Γ_x is the width for the primary process ($\Gamma_{\alpha'}$ in the case of fluorine, Γ_γ in all the others), and Γ is the width for all competing processes. Y is the thick target yield, λ is the wave-length of the incident protons at resonance, and ϵ is the stopping cross section of the target for protons per disintegrable nucleus. Values of ϵ for air are given as a function of proton energy in Livingston and Bethe.[12] We take the stopping power of CaF_2 to be 1.97 per F^{19} nucleus and that of LiOH to be 2.03 per Li^7 nucleus.

The proton width Γ_p and the specific reaction width Γ_x are given in terms of γ and Γ by the equations

$$\Gamma_p=\tfrac{1}{2}\Gamma(1\pm(1-4\gamma/\Gamma)^{\frac{1}{2}}), \tag{80}$$

$$\Gamma_x=\tfrac{1}{2}\Gamma(1\mp(1-4\gamma/\Gamma)^{\frac{1}{2}}). \tag{81}$$

These equations do not determine Γ_p and Γ_x unambiguously. For example, if $\gamma\ll\Gamma$ as in all the cases under discussion, the smaller of Γ_p and Γ_x is then equal to γ and the greater to Γ. Additional arguments must then be advanced to resolve the ambiguity. An additional uncertainty arises from the fact that $\omega\gamma$ rather than γ is actually found in the yield measurements. The statistical factor is given by

$$\omega=2J+1/(2s+1)(2i+1), \tag{82}$$

where s = total momentum of target nucleus ($\frac{3}{2}$ for Li^7 and Be^9, 0 for C^{12}, $\frac{1}{2}$ for C^{13} and F^{19}), i = spin of incident particle ($\frac{1}{2}$ for proton), and J = total angular momentum of compound nu-

[37] W. A. Fowler, E. R. Gaerttner, and C. C. Lauritsen, Phys. Rev. **53**, 628 (1938); R. B. Roberts and N. P. Heydenburg, Phys. Rev. **53**, 374 (1938); L. R. Hafstad and M. A. Tuve, Phys. Rev. **48**, 306 (1935).

cleus. In the cases under discussion, ω varies from $\frac{1}{8}$ to slightly over unity.

The yield determinations of $\omega\gamma$ and the excitation curve determinations of Γ are summarized in Tables V and VI. The information concerning the many resonances in the case of $F(p\alpha', \gamma)$ has been obtained by correcting the absolute yields at 338 and 862 kev given in the paper by Streib, Fowler, and Lauritsen[18] to fit the newer and more accurate values obtained in these experiments. For other resonances we have employed the relative yields of Bennett *et al.*,[38] to calculate the absolute yields. The resonance widths given by Bennett *et al.* are tabulated.

In all but the case of $F^{19}(p\alpha', \gamma)$, the radiation comes from the compound nucleus. The observed widths, Γ, are large compared to possible radiation breadths, and so the widths must be due to proton re-emission or to competing particle reactions. In the cases of $C^{12}(p\gamma)$, $C^{13}(p\gamma)$ no competing heavy particle reactions are possible. Hence $\Gamma_p \sim \Gamma$ and $\Gamma_\gamma \sim \gamma$. A similar result holds in the $Li^7(p\gamma)$, since the energetically possible reaction $Li^7(p\alpha)\alpha$ does not show resonance at 440 kev and presumably does not compete in the disintegration of this state of Be^8. The $Be^9(p\gamma)$ reaction is complicated in that two competing reactions $Be^9(p\alpha)Li^6$ and $Be^9(pd)Be^8$ are each about 10 percent as strong as the elastic scattering reaction $Be(pp)Be^9$ near 1 Mev.[39] We make no correction for these reactions, so that in this case our estimates of Γ_p and Γ_γ may be in error from this source by as much as 20 percent. In the $F^{19}(p\alpha', \gamma)$ case the $\omega\gamma$ are small compared to the observed Γ. The primary process is the emission of a short range α-particle. Hence either $\Gamma_p/\Gamma_{\alpha'}$ or $\Gamma_{\alpha'}/\Gamma_p$ is small with $\gamma=\Gamma_p$ and $\Gamma=\Gamma_{\alpha'}$ in the first case and $\gamma=\Gamma_{\alpha'}$ and $\Gamma=\Gamma_p$ in the second. Experimentally the γ increase markedly with energy and the Γ do not. Hence, it is most reasonable to accept the first case, the rapid variation of γ then being attributed to the rapid increase of Γ_p with increasing bombarding energy resulting from the Gamow factor. The alpha-particle energy does not vary greatly with E_p, and so $\Gamma=\Gamma_{\alpha'}$ is relatively less sensitive to this energy.

[38] W. E. Bennett, T. W. Bonner, C. E. Mandeville, and B. E. Watt, Phys. Rev. **70**, 882 (1946).

[39] R. G. Thomas, W. A. Fowler, and C. C. Lauritsen, Bull. Am. Phys. Soc. UCLA Meeting (January 1948).

The values for Γ_p which have been obtained in the two types of reactions under consideration depend critically on the proton energy because of the barrier penetration factors which they contain. If the angular momentum of the protons is known (*s*-wave, *p*-wave, *d*-wave, etc.) this factor can be estimated. We employ the results given in an accompanying article by Christy. In general, the angular momentum of the protons producing the resonance is not known, so that corrections have been made for *s*, *p*, and *d* waves. The corrections have been made in such a way as to give the width without barrier (Γ_0) at an energy of 1-Mev energy for the proton. In this way the linear dependence of Γ_p on the velocity of the proton is also eliminated. The results are given in Tables V and VI. Of course the values obtained from $\omega\gamma=\omega\Gamma_p$ contain the statistical factor ω. This fact makes it difficult to assign definite angular momentum values to the incident particles. In addition, the widths without barrier can be expected to vary by about a factor of 10 or even more because of specifically nuclear factors. Some decrease in widths with increasing mass number A and with increasing excitation of the compound nucleus is also to be expected. The values given in Tables V and VI show considerable variation, and it is not possible at the present time to make definite assignments of the angular momentum of the incident particles and of the spin of the compound nucleus on the basis of these considerations.

The radiation widths determined experimentally can be compared with those to be expected for electric dipole, electric quadripole, and magnetic dipole radiation when the energy is known. The radiation widths for these various types of radiation are given by

electric 2^l-pole:

$$\Gamma_\gamma=\frac{4}{3}\left(\frac{r}{r_0}\right)^{2l}\left(\frac{\alpha h\nu}{mc^2}\right)^{2l+1}mc^2,$$

magnetic dipole:

$$\Gamma_\gamma=\frac{1}{3}\alpha\left(\frac{\mu}{\mu_n}\right)^2\left(\frac{m}{M}\right)^2\left(\frac{h\nu}{mc^2}\right)^3mc^2, \tag{83}$$

where er^l is the matrix element for the electric 2^l-pole radiation, μ is the radiation magnetic

moment, μ_n is the nuclear magneton, α is the fine structure constant, m/M is the ratio of electron and proton masses, and r_0 is the classical electron radius taken as a convenient unit of length because it is approximately equal to the range of nuclear forces. For comparison with the experimental values it is convenient to determine r/r_0 and μ/μ_n which are given numerically by

$$\begin{aligned}
&\text{electric dipole:} && \frac{r}{r_0}=0.7\Gamma_\gamma^{\frac{1}{2}}(h\nu)^{-\frac{3}{2}},\\
&\text{electric quadripole:} && \frac{r}{r_0}=7\Gamma_\gamma^{\frac{1}{2}}(h\nu)^{-5/4},\\
&\text{magnetic dipole:} && \frac{\mu}{\mu_n}=19\Gamma_\gamma^{\frac{1}{2}}(h\nu)^{-\frac{3}{2}},
\end{aligned} \tag{84}$$

for $\Gamma\gamma$ in ev and $h\nu$ in Mev.

In further discussion we will consider separately the various reactions on which we have made experimental measurements of Γ_γ and Γ_p. The selection rules for the various types of radiations, which we will use in the discussion, are

electric dipole:

$\Delta J=0, \pm 1$ parity changes,

electric quadripole:

$\Delta J=0, \pm 1, \pm 2$ parity does not change, (85)

magnetic dipole:

$\Delta J=0, \pm 1$ parity does not change.

$C^{12}(p\gamma)$ *and* $C^{13}(p\gamma)$

These reactions are considered first because of their simplicity in that proton and gamma-ray emission alone compete. The large observed widths must be attributed to proton emission and when corrected for s-wave barrier factors give widths without barrier of the order of 1 Mev and still greater for p- and d-wave corrections. The maximum width for proton re-emission can be estimated from the time required for the proton to cross the compound nucleus without collision. This yields several Mev for 0.5-Mev protons incident on carbon nuclei. Collisions with nuclear matter will increase the time and decrease Γ_p. Hence it is reasonable to assume that these reactions are due to s-wave protons. It would seem reasonable too, that the width without barrier should be greater for C^{12}, where all the particles have saturated forces (α-particle model) and thus will not interact strongly with the incident proton, than for C^{13} with the unsaturated extra neutron which will certainly exert strong forces on the incident proton.

In the case of C^{12}, which has zero spin and even parity, the compound nucleus, N^{13}, will have $J=\frac{1}{2}$ and even parity. The statistical factor will be equal to unity. The ground state of N^{13} is probably $J=\frac{1}{2}$ with odd parity so that electric dipole radiation is allowed. The radiation breadth, $\Gamma_\gamma=0.63$ ev, is not unreasonable for such radiation when the gamma-energy is 2.3 Mev, since we find $r=0.16r_0$ from Eq. (80).

In the case of C^{13}, which has spin $\frac{1}{2}$ and odd parity, the compound nucleus N^{14} will have odd parity and spin 0 or 1. Hence $\omega=\frac{1}{4}$ or $\frac{3}{4}$. The ground state of N^{14} has even parity and spin 1. For either compound state electric dipole radiation is allowed. The width for the transition to the ground state ($h\nu=8.1$ Mev) is $\sim 7.5/\omega$ ev $=30$ or 10 ev, so that in this case $r=0.17r_0$ or $0.10r_0$. If the transition to the intermediate state ($h\nu=2.3$ Mev) is electric dipole and of width $\sim(7.5/\omega$ ev), then $r=1.1r_0$ or $0.6r_0$. This large dipole moment is somewhat unusual in nuclei, and it indicates that a more careful determination of the intensity of the 2.3-Mev and 5.8-Mev lines relative to the 8.1-Mev line is necessary.

The $C^{12}(p\gamma)$ and $C^{13}(p\gamma)$ reactions are of interest because they are among the reactions in the carbon-nitrogen cycle proposed by Bethe[40] as the source of stellar energies. We can assume that the carbon-hydrogen reactions at stellar temperatures are due to the tails of the resonances observed in these investigations in order to estimate the cross sections for these reactions. It is true that other resonances, particularly at low energy, would affect the stellar results considerably and might not be observable in the laboratory. Resonances at still higher energies might interfere constructively or destructively at stellar temperatures with the effects of those near 0.5 Mev. We have observed no other strong res-

[40] H. A. Bethe, Phys. Rev. 55, 434 (1939).

onances up to 1.3 Mev in bombarding energy. Nevertheless, the order of magnitude of the cross section at stellar temperature can be obtained. The expression used by Bethe for the cross section at stellar temperatures is

$$\sigma=\frac{\pi R^2}{2E}\omega\Gamma_\gamma e^{-2G}=\pi\lambda^2\left(\frac{MR^2}{\hbar^2}\right)\omega\Gamma_\gamma e^{-2G}, \quad (86)$$

where R is the radius of the compound nucleus, E the energy of the incident and target nucleus in the center of mass system, and e^{-2G} is the Gamow factor arising from the dependence on energy of Γ_p which does not appear explicitly in the expression. The dispersion formula predicts

$$\sigma=\pi\lambda^2\omega\Gamma_\gamma\frac{\Gamma_p}{E_R{}^2} \quad (87)$$

for the effect of a resonance at E_R. The proton width at stellar temperatures, Γ_p, must be computed from that at resonance by employing the Gamow factor for barrier penetration so that the two expressions are somewhat similar. Most important, however, is the use by Bethe of the expression

$$\frac{E_R{}^2}{\hbar^2/MR^2}\sim\frac{E_R{}^2}{3}\sim 0.1 \text{ Mev}$$

for Γ_p corrected for the barrier factor. This is considerably smaller than the width without barrier we have computed from the observations, and when the Gamow factors are more exactly computed[41] the cross sections are found to be about 40 times that estimated by Bethe for $C^{13}(p\gamma)$. The corrected lifetimes for C^{12} and C^{13} in the sun are thus 6×10^4 and 7×10^3 years, and the stellar abundances are calculated to be in the ratio 9 to 1. The disagreement with the terrestial abundance $\sim$90 to 1 is not unexpected in view of the simplifications of the theory. Although the situation in regard to the nitrogen-proton reactions is not very satisfactory, it is well to note at this point that these measurements indicate a relative stellar abundance of 3×10^3 for C^{12} and N^{15}, using the 20 year half-life computed for N^{15} by Bethe[42] from measurements by Holloway and Bethe[43] on $N^{15}(p\alpha)$. The yield of the $N^{14}(p\gamma)$ reaction reported by Curran and Struthers[44] is very low, but there seems to be little reason why it should differ considerably from that for $C^{12}(p\gamma)$. Our results for the C^{12} reactions indicate that the $(p\gamma)$ reactions in the sun are 3×10^{-4} times as probable as the $(p\alpha)$ reactions rather than 10^{-6} as indicated by Bethe.[42] Hence the N^{15}/C^{12} abundance in the sun should be 3×10^{-4} which is to be compared with 12×10^{-4} calculated from $N^{14}/C^{12}\sim0.33$ and $N^{15}/N^{14}=0.0038$. Thus there may exist no great discrepancy between isotopic abundances found terrestially and those calculated for the sun on the basis of the carbon-nitrogen cycle and the extrapolation of laboratory yields to very low bombarding energies. We propose to make additional measurements on the nitrogen-proton reactions in the near future.

$Li^7(p\gamma)$

The proton width without barrier for this reaction is considerably smaller than those for C^{12} and C^{13} if we assume the resonance at 439 kev is due to s-capture. This may arise from the high excitation in Be^8, the compound nucleus. At high excitation we can expect small level separations and small widths if decay by high energy particles is forbidden. The result for p-capture seems somewhat more reasonable. Since Li^7 has spin $\frac{3}{2}$ and odd parity the compound state in Be^8 has even parity and spin 0, 1, 2 or 3 for p-capture. We can forbid α-emission, as observed, by assigning spin 1 or 3 to that state. For spin 1 the radiation to the ground state of Be^8 (0, even) is electric quadripole or magnetic dipole. The statistical factor is $\frac{3}{8}$ and $\Gamma_\gamma=24$ e-volts. In this case $R=0.4r_0$ for electric quadripole or $\mu=0.6\mu_n$ for magnetic dipole radiation. In the past it has been assumed that the reaction was due to s-capture and α-emission was forbidden because either compound state (spin 1 or 2) has odd parity. For spin 1 the radiation is electric dipole, $\omega=\frac{1}{8}$, and $\Gamma_\gamma=70$ e-volts. This gives $R=0.08r_0$ for electric dipole radiation. It is not possible at present to distinguish between the two hypotheses. The isotropic angular distri-

[41] J. O'Reilly and R. F. Christy, Bull. Am. Phys. Soc. UCLA Meeting (January 1948).

[42] H. A. Bethe, Astrophys. J. **94**, 37 (1940).

[43] M. G. Holloway and H. A. Bethe, Phys. Rev. **57**, 747 (1940).

[44] S. C. Curran and J. E. Strothers, Nature **145**, 224 (1940).

bution of the radiation follows directly if s-capture is assumed, but it cannot be ruled out for p-capture without special assumptions concerning the state of Be^8. Further investigation of the resonance scattered protons[8] will be necessary to establish the character of the state of Be^8 which enters into the reaction.

$Be^9(p\gamma)$

The widths for proton re-emission in this case seem most consistent with those observed for C^{12} and C^{13} if one assumes the 988-kev resonance to be due to p-capture and that at 1077 kev to be due to d-capture. The assignment of p-capture to the state at 988 kev is consistent with the results of Rubin[45] on the angular distribution of scattered protons at this resonance, but Rubin's results do not critically determine the angular momentum of the incident wave. Since Be^9 presumably has odd parity, the two states at 988 kev and 1077 kev will have even and odd parity, respectively. The capture of p protons by Be^9 (spin $\frac{3}{2}$) results in states of B^{10} of spin 0, 1, 2, or 3. All of these can give electric quadripole radiation to the ground state of B^{10} (1, even), and the first three can give magnetic dipole. The reaction $Be^9(pd)Be^8$ probably competes[39] in the decay of this state, and since the deuterons are of low energy it is most reasonable to assume that they escape as an s-wave making the 988-kev resonance a $J=1$, even state. We then have $\omega=\frac{3}{8}$ and $\Gamma_\gamma=33$ e-volts. For electric quadripole radiation we find $r=1.4r_0$ while for magnetic dipole we have $\mu=5.5\mu_n$.

The capture of d-protons by Be^9 results in states of B^{10} of spin 0, 1, 2, 3, or 4. The narrow state at 1077 kev shows no evidence for deuteron or alpha-particle disintegration, and the radiation width to the ground state of B^{10} is very small (<0.1 ev). The observed transition with a width of 0.77 e-volt is to an intermediate state of B^{10}. These results will be expected if a J-value of 3 or 4 is assigned to the level. The deuteron or alpha-emission would require very high relative angular momenta in these cases, and the radiation to the ground state could not be electric dipole, electric quadripole, or magnetic dipole. A suitable assignment of spin and parity to the intermediate state of B^{10} at 0.7 Mev would make allowed gamma-ray transitions to this state consistent with the observed breadth of 0.77 ev ($r=0.04r_0$ for electric dipole radiation).

$F^{19}(p\alpha', \gamma)$

This reaction has recently been discussed by Schiff,[46] who assumes $F^{19}(J=\frac{1}{2})$ to have odd parity and then concludes that the gamma-ray emitting state in O^{16} at 6.3 Mev has $J=1$ and even parity, and the pair emitting state at 6.1 Mev has $J=0$ and even parity. A most striking feature of the disintegration of F^{19} by protons is the small probability for emission of long range alphas leaving O^{16} in the ground state, and for emission of short range alphas leaving O^{16} in the pair emitting state. These reactions are the order of several percent of the reaction in which short range alphas are emitted leaving O^{16} in the gamma-ray emitting state. From the observed widths, as given in Table VI, we would be inclined to attribute the strong gamma-radiation to s- and p-capture and the pair and long range alpha-emission to d-capture. This is consistent with the results of Rubin,[45] who finds that the angular distribution of long range alphas at 1350 kev requires at least d-capture. It is not possible to forbid long range alpha-particle emission for both s and p incident protons on the basis of the total angular momentum—parity selection rule. The assumption that both orbital and spin angular momentum must be conserved in the reaction makes the results somewhat more plausible. For example, if one assumes the ground state of F^{19} to be mainly a $^2S_{\frac{1}{2}}$ odd state, then none of the singlet states formed by proton bombardment has the proper parity and angular momentum to permit long range alpha-emission (or short range alpha-emission leading to the pair emitting state of O^{16} if this is assumed to have $J=0$ and even parity). Furthermore, all the triplet states will require interchange of spin and orbital momentum. Long range alpha-emission and pair emission will thus be weak on the assumption made above. On the other hand, the assignment of $J=1$ and odd parity to the gamma-ray emitting state of O^{16} will permit the triplet state formed by s-capture to result in

[45] S. Rubin, Phys. Rev. (in publication).

[46] L. I. Schiff, Phys. Rev. **70**, 891 (1946).

s-wave alpha-emission and thus the transition will be a probable one. It is hoped that more detailed angular distribution measurements will help clarify the situation in these reactions.

c. Summary

The measurements of the yield and energy of the gamma-radiation produced in nuclear reactions and of the excitation curves for the production of the is radiation leads to considerable empirical knowledge concerning the excited states of nuclei. At the present time the knowledge is not sufficient to make definite assignments concerning the spectroscopic characteristics of these states. The problems will not be solved until complete information on all possible competing modes of decay of the excited states has been obtained. In this laboratory[39,45] and in others attempts are being made to obtain this information at the present time.

In conclusion we wish to thank Professor R. F. Christy for many valuable discussions of the material presented here. The experimental work was supported in part by the Office of Naval Research.